DISSERTATIONS IN
FORESTRY AND
NATURAL SCIENCES

Joakim Riikonen

Modification, Characterization and Applications of Mesoporous Silicon-Based Drug Carriers

Publications of the University of Eastern Finland
Dissertations in Forestry and Natural Sciences

UNIVERSITY OF
EASTERN FINLAND

JOAKIM RIIKONEN

Modification, characterization and applications of mesoporous silicon-based drug carriers

Publications of the University of Eastern Finland
Dissertations in Forestry and Natural Sciences
No 84

Academic Dissertation
To be presented by permission of the Faculty of Science and Forestry for public examination in the Auditorium L22 in Snellmania Building at the University of Eastern Finland, Kuopio, on September, 14, 2012, at 12 o'clock noon.

Department of Applied Physics

Kopijyvä Oy
Kuopio, 2012
Editors: Prof. Pertti Pasanen
Prof. Pekka Kilpeläinen, Prof. Matti Vornanen

Distribution:
Eastern Finland University Library / Sales of publications
julkaisumyynti@uef.fi
www.uef.fi/kirjasto

ISBN: 978-952-61-0894-0 (printed)
ISSNL: 1798-5668
ISSN: 1798-5668
ISBN: 978-952-61-0895-7 (pdf)
ISSN: 1798-5676

Author's address: University of Eastern Finland
Department of Applied Physics
P.O.Box 1627
70211 KUOPIO
FINLAND
email: joakim.riikonen@uef.fi

Supervisors: Professor Vesa-Pekka Lehto, Ph.D.
University of Eastern Finland
Department of Applied Physics
P.O.Box 1627
70211 KUOPIO
FINLAND
email: vesa-pekka.lehto@uef.fi

Docent Jarno Salonen, Ph.D.
University of Turku
Department of Physics and Astronomy
20014 TURKU
FINLAND
email: jarno.salonen@utu.fi

Reviewers: Professor Mika Lindén, Ph.D
Ulm University
Institute of Inorganic Chemistry II
Albert-Einstein-Allee 15
89069 ULM
GERMANY
email: mika.linden@uni-ulm.de

Professor Sami Franssila, Ph.D
Aalto University
Department of Material Science and Engineering
P.O.Box 1600
00076 ESPOO
FINLAND
email: sami.franssila@aalto.fi

Opponent: Professor Leigh Canham, Ph.D
pSivida
Geraldine Road
WR143SZ MALVERN
UNITED KINGDOM
email: lcanham@psivida.com

ABSTRACT

Many new drug molecules suffer from poor bioavailability. The majority of new drug candidates are poorly soluble which can severely affect their bioavailability. For example, peptide drugs have great potential in the treatment of illnesses but so far, their commercial success has been restricted largely because of their short duration of activity.

Mesoporous materials represent a nanotechnological solution to the current problems in drug delivery. Improved dissolution of poorly soluble drug or a sustained release of peptides can be provided by loading drugs into small pores which are only a few nanometers wide.

The successful development of a mesoporous drug carrier involves both the production of the porous material and the design of the appropriate surface chemistry. Furthermore, it is essential to make a detailed characterization of the properties of the carrier and the drug loaded inside the pores. Finally, the delivery of the drugs in an active form needs to be assessed *in vivo* and the safety of the material has to be confirmed.

The present work addresses all of the above mentioned aspects of drug carrier development. More specifically, the development of a method for controlling the pore size by annealing of porous silicon is described. In addition, surface stabilization by oxidation was studied to produce inert carrier surfaces with a minimal effect on the pore structure. This work also addressed the characterization of mesoporous materials by development of a novel method for quantitative determination of pore morphology of an ordered mesoporous silica material. Furthermore, the physical state of a model drug, ibuprofen, in the pores of porous silicon was studied. This study revealed the effect of pore size and surface chemistry on the crystallinity of the drug. Finally, delivery of a peptide from a porous silicon carrier was studied with animal models. A sustained release of peptide in an active form was achieved without any signs of inflammatory reactions.

Universal Decimal Classification: 546.28, 620.3, 62-405.8, 661.8'065
National Library of Medicine Classification: QT 36.5, QT 37, QV 785
Medical Subject Headings: Biomedical and Dental Materials; Biological Availability; Nanotechnology; Nanostructures; Porosity; Silicon; Drug Carriers; Drug Delivery Systems; Surface Properties; Ibuprofen; Peptides; Models, Animal
Yleinen suomalainen asiasanasto: materiaalitiede; nanotekniikka; nanomateriaalit; huokoisuus; pii; lääkeaineet – annostelu; ibuprofeeni; peptidit; pintakemia

Preface

The work presented here has been carried out during the years 2007 – 2012. These years have been the years of numerous mergers in Finnish universities and therefore the names of the universities and departments have been unstable. Nevertheless, this work was carried out in two locations which currently bear the names: Department of Physics and Astronomy in University of Turku and Department of Applied Physics in University of Eastern Finland. Funding from National Doctoral Programme in Nanoscience, the Academy of Finland, the University of Eastern Finland and ultimately the taxpayers is sincerely acknowledged.

I have always considered it to be a privilege to work in science and even to be paid for it. Conducting research in mesoporous materials and drug delivery has been truly fascinating, providing me with constant challenges and new things to be learned. The occasional eureka moments have overshadowed the far more numerous moments of frustration when nothing seemed to work. This work has also taught me how vast is our knowledge of the world around us and how little one person can know.

Undoubtedly, this work could not have been carried out by a single person alone. Scientifically, researchers are always standing on the shoulders of giants but even more importantly on the shoulders of millions of past and present peers who have contributed countless hours to generate the current knowledge. Only because of these people has it been possible for me to gather the drops of information presented here.

On a personal level, people who have directed and supported my journey and have encouraged good ideas and repressed the bad ones are the ones who have made this possible, and towards whom I feel the most gratitude.

First and foremost, I would like to thank my primary supervisor Professor Vesa-Pekka Lehto for the opportunity to

work in his group during the past eight years and especially for believing in my abilities and for giving me the guidance and responsibilities required for professional growth. I am also grateful to my supervisor docent Jarno Salonen for his support, all the corridor meetings, "rooftop reprimands" and for an introduction to the idea-rich and messier side of science. I would also like to thank the staff and management of the departments and faculties in which I have been working during these years. All the co-authors of the original publications are acknowledged for their important scientific contributions. The valuable help with the language of the thesis provided by Lucia Podracká and Ewen MacDonald is highly appreciated.

I would like to thank the examiners of this thesis Mika Lindén and Sami Franssila for their critical but constructive comments. I am deeply honored that Professor Leigh Canham has agreed to be the opponent of my dissertation. This thesis would not have seen the daylight without his highly influential research into porous silicon.

During the years, I have had pleasure to work with many colleagues who are truly responsible for friendly, helpful and inspiring working environments. Before joining the Teollisuusfysiikka-team, I had no idea that it was legal to have so much fun at work. I would also like to thank Jukka Laakkonen for his indispensable help during and after the construction of our new laboratory in Kuopio. All the members in HUMALA, PEPBI, COMPSi, NAMBER and PSindustry projects in Helsinki, Joensuu, Kuopio, Lappeenranta and Turku are acknowledged for the fruitful and enjoyable collaboration. I would also like to thank Marianna Kemell for patiently taking SEM images of our samples, including the SEM images in this thesis. In addition to their scientific contributions, I am very grateful to Juha Mönkäre and Miia Kilpeläinen for their help in acclimatizing me to Kuopio and for the important contacts they helped me to acquire.

This work would not have been possible without contribution to the less scientific parts of my life. I am very thankful to Kimmo Lehtinen and Jorma Roine for the

fellowship, which is not broken, starting from the first days of our physics studies. I'm also grateful to all my other friends for all the fun outside science. Special thanks go to Vesa Aaltonen for the years of friendship and the many unforgettable challenges we have tackled together.

My relatives and my godparents Marra and Sauli have always been a great support for me for which I am very grateful. I will never be able to thank enough my parents Kaisa and Seppo and my sister Henna-Juulia for all that they have done for me and for all that they are for me. Finally, this list would not be complete if I did not express my deepest gratitude to my beloved Lucia; neither am I complete without you.

Kuopio August 17, 2012 *Joakim Riikonen*

LIST OF ABBREVIATIONS

AA	as-anodized
Al-SBA-15	Aluminum containing SBA-15
C	Carbon
DSC	Differential scanning calorimetry
e^-	Electron
EPR	Electron paramagnetic resonance spectroscopy
FTIR	Fourier transformation infrared spectroscopy
GhA	Ghrelin antagonist, peptide
H	Hydrogen
h^+	Hole (empty electron state in valence band)
H_2O_2	Hydrogen peroxide
HF	Hydrofluoric acid
HNO_3	Nitric acid
HPLC	High performance liquid chromatography
MCM-41	Mobil composition of matter no. 41, an ordered mesoporous silica
NMR	Nuclear magnetic resonance spectroscopy
O	Oxygen
PSi	Porous silicon
S1, S2, S3	Sample 1, 2 and 3. Oxidized porous silicon samples in publication II
SBA-15	Santa Barbara amorphous 15, an ordered mesoporous silica
SEM	Scanning electron microscopy
Si	Silicon
$Si\text{-}H_x$	Silicon hydride
SiF_6^{-2}	Silicon hexafluoride
SiO_2	Silicon dioxide, silica
TC	Thermally carbonized
TCPSi	Thermally carbonized porous silicon
TEM	Transmission electron microscopy
TG	Thermogravimetry
THCPSi	Thermally hydrocarbonized porous silicon
TO	Thermally oxidized

TO120	Thermally oxidized (300 °C, 120 min) porous silicon
UV/VIS	Ultraviolet/visible light
XRD	X-ray diffraction

LIST OF SYMBOLS

ΔH	Melting enthalpy
Δh	Specific melting enthalpy
ΔT	Melting point depression
δ	thickness of non-crystalline delta layer
κ	Curvature
A	Surface area
D	Pore diameter
K	Constant in Gibbs-Thomson equation
R_c	Crystal radius
R_p	Pore radius
t	Time
V	Volume

LIST OF ORIGINAL PUBLICATIONS

This thesis is based on data presented in the following articles, referred to by the Roman numerals I-V.

I Salonen J, Mäkilä E, Riikonen J, Heikkilä T and Lehto V-P, Controlled enlargement of pores by annealing of porous silicon, *Physica Status Solidi 206: 1313-1317, 2009.*

II Riikonen J, Salomäki M, van Wonderen J, Kemell M, Xu W, Korhonen O, Ritala M, MacMillan F, Salonen J and Lehto V-P, Surface chemistry, reactivity and pore structure of porous silicon oxidized by various methods, *Langmuir 28: 10573-10583, 2012*.

III Riikonen J, Salonen J, Kemell M, Kumar N, Murzin D, Ritala M and Lehto V-P, A novel method of quantifying the u-shaped pores in SBA-15, *Journal of Physical Chemistry C 113: 20349-20354, 2009.*

IV Riikonen J, Mäkilä E, Salonen J and Lehto V-P, Determination of the physical state of drug molecules in mesoporous silicon with different surface chemistries, *Langmuir: 25, 6137-6142, 2009.*

V Kilpeläinen M*, Riikonen J*, Vlasova M A, Huotari A, Lehto V-P, Salonen J, Herzig K-H and Järvinen K, In vivo delivery of a peptide, ghrelin antagonist, with mesoporous silicon microparticles, *Journal of Controlled Release 137: 166-170, 2009*. (* Authors share an equal contribution)

AUTHOR'S CONTRIBUTION

I The author prepared part of the samples and performed part of the nitrogen sorption measurements.

II The author planned the study and prepared all the samples. He also did all the experiments and data analysis related to XRD, FTIR, ITMC and gas sorption (except part of the gas sorption measurements). The author was the principal writer of the manuscript.

III The author planned the study and did all the measurements and data analysis, except SEM imaging. He was the principal writer of the manuscript.

IV The author participated in the planning of the study. The author performed all the experimental work and was the principal writer of the manuscript.

V The author developed the loading method, prepared all the peptide loaded PSi samples and performed the measurements and data analysis related to TG and gas sorption. He participated in writing the manuscript.

Contents

1 Introduction

A large number of drugs encounter serious difficulties in their delivery. In order for a drug to exert a therapeutic effect, it needs to be delivered to the site of action at a sufficient concentration and to be present for an adequate length of time. Poorly soluble and peptide drugs are types of drugs that often face difficulties meeting these demands.

The poor solubility of drugs is a serious and an increasing problem in pharmaceutical industry. As many as 70 % of new drug candidates suffer from poor solubility [1] and poor solubility of drugs frequently leads to low bioavailability. In order to increase the bioavailability, higher doses could be administered but this strategy may cause other problems such as toxicity, difficulties in formulation and high costs [2].

Several approaches have been developed to overcome poor solubility [2]. Sometimes it is possible to chemically modify the molecule or produce a salt form to obtain a more soluble form [2]. However, these methods are not always successful or desirable, and therefore physical methods are often used instead. These physical methods include forming a metastable polymorph, creating an amorphous form or reducing the particle size down to the nanoparticle range [3]. These approaches often suffer from poor physical stability [3]. It is also possible to utilize excipients to improve dissolution properties. Solid dispersions and co-crystals can be formed or the drug can be complexed with cyclodextrins [3-5]. These formulations are usually very specific for each drug molecule and thus considerable formulation development has to be done for each individual molecule [3-5]. In addition, the loading degrees achieved with these methods are typically low and their production can be complicated [2, 6].

Peptide/protein drugs also often encounter serious delivery problems. Peptides and proteins are abundant in living

organisms participating in various functions and diseases. Therefore, peptide/protein drugs hold considerable promise for the treatment of various illnesses. Despite their potential, only a few peptide/protein drugs have reached the market, often owing to serious difficulties in their delivery [7]. The two main limitations in peptide/protein delivery are poor absorption through non-invasive routes, and their short duration of activity which is caused by the rapid renal clearance and enzymatic degradation [7, 8]. Repeated injections are almost invariably used to overcome these limitations, resulting in poor patient compliance [7].

The most widely studied sustained release carriers of peptides/proteins are various polymer-based formulations. In addition, carriers such as liposomes and solid lipid nanoparticles have been evaluated [9]. However, these formulations have usually low loading degrees which make them an unlikely solution for drugs which need to be administered at high doses [7, 9]. Furthermore, the polymer formulations suffer from stability issues, difficulties in manufacturing and their large particle size requiring painful injections [7].

Mesoporous materials are potential drug carriers [10]. The research in this field is rapidly increasing. According to the Web of Science, over 1600 articles have been published in this field since year 2000 with 60 % of the articles appearing during the last 3 years.

Mesoporous materials consist of pores with diameters in the range of 2 nm–50 nm, are typically highly porous and have large specific surface areas. These structures have a high capacity to absorb drug molecules into their pore structures achieving high drug loading degrees.

The delivery of poorly soluble and peptide drugs from mesoporous materials can resolve many of the problems associated with these molecules. For poorly soluble drugs, an enhanced release rate can be achieved by confining the drug into mesopores. The improved release is a result of changes in the physical state of loaded drugs and their large surface areas

[10]. Not only is the release rate enhanced but also the state of the drug is efficiently stabilized. Furthermore, it has been shown that this method can be extended to a wide variety of poorly soluble drugs [11]. There is no need to tune the carrier according to the properties of the drug, provided that one can ensure chemical compatibility between drug and carrier. In addition, loading of the carrier is uncomplicated, at least on a laboratory scale, and can be performed at room temperature.

The use of mesoporous materials as carriers for peptides/proteins is clearly an emerging and promising application. One potential benefit of the carrier is a sustained release resulting from attachment of molecules onto the surface and diffusion limitations. In addition, the pore structure might be able protect the molecules from enzymatic degradation prior to release since the enzymes cannot gain access into the pores.

Successful preclinical development of a mesoporous carrier involves the production of carrier with a suitable pore structure and appropriate surface chemistry. In order to predict and understand the behavior of the carrier, the properties such as pore morphology have to be extensively characterized. It is equally important to understand the properties of drugs in the pores. Finally, the release and activity of the loaded drug have to be evaluated as well as the safety of the material.

All of the above-mentioned aspects in development of mesoporous carriers are discussed in the present work. The experimental work in the original publications begins with the production of porous silicon, specifically with modifications to the pore structure (I) and surface stabilization by oxidation (II). A novel method was developed for the characterization of mesoporous SBA-15; this method was capable of quantifying u-shaped pores in the material (III). In addition, a study into the characterization of crystalline ibuprofen in mesopores was conducted (IV). Finally, it was shown that porous silicon could be applied in sustained delivery of peptides *in vivo* (V).

2 Literature review

Drug delivery by mesoporous materials including all related topics is a very wide subject addressed by thousands of scientific articles published during the last two decades. Therefore, this review does not attempt to be an exhaustive survey of the literature, but rather to introduce readers to the subject and to provide a comprehensive account on the phenomena and methods that are related to the topic. The emphasis is on the mesoporous materials used in the experimental part, mainly porous silicon, the methods used for characterization, and the delivery of peptides and poorly soluble drugs.

The first part of the chapter addresses the production and properties of porous silicon and ordered mesoporous silicas. Subsequently, the characterization of these materials is discussed. The last part of the chapter surveys drug delivery applications, starting from the production of loaded carriers to the information that can be obtained about them by characterization and, finally, to the actual drug release from the carriers.

2.1 MESOPOROUS MATERIALS

Mesoporous materials have attracted significant and ever-increasing research interest since the early 1990's. They have provided new possibilities over a wide range of applications not only in areas from catalysis to electronics but also in drug delivery by allowing manipulation of the internal structure of materials in a nanometer range and by providing a large area to promote various surface–guest molecule interactions.

By definition mesopores are pores with a diameter between 2–50 nm, while smaller pores are called micropores and the

larger pores are termed macropores [12]. The term nanopore is also sometimes used to describe mesopores as well as large micropores and small macropores, but this does not have a generally accepted definition. In addition to the pore size, the most important properties of the mesoporous materials include their ability to control the pore size and wall thickness, the regularity of their structure, and high surface area.

There are several types of mesoporous materials such as mesoporous carbon, polymers and various metal oxides [13]. The most studied mesoporous materials in drug delivery applications are silicon based: porous silicon (PSi) and porous silica. These two materials are also those used in the present study.

2.1.1 Porous silicon

As with many other scientific discoveries, such as penicillin or Teflon, PSi was discovered by accident. It was first produced in Bell Labs in 1956 by Arthur and Ingeborg Uhlir while studying electrochemical etching of silicon and germanium, aiming at the production of smooth surfaces [14, 15]. They noticed that a film was produced on silicon with certain etching parameters, but they were not aware of the porous nature of the film. It was only 15 years later when the true nature of this film was discovered [16]. Very little research was conducted PSi during the 1970's and 1980's. However, after an incubation of 20 years, wide scientific interest in PSi was triggered by Leigh Canham's influential article in 1990, reporting the photoluminescence of PSi at room temperature [17]. Further interest and possibilities for a new range of applications emerged after another pioneering article by Canham reported that porosification of silicon could affect the biological behavior of the material [18].

The most widely utilized method of producing PSi for drug delivery applications is electrochemical etching because it provides the best control over the pore structure [19]. However, recent progress in other methods, such as stain etching [20] or metal assisted etching [21], should not be ignored, since these

techniques might provide a more economical way for mass production of PSi by allowing utilization of a low-cost raw material and larger batch sizes.

The electrochemical etching of silicon is performed in an electrochemical cell where a crystalline silicon wafer acts as an anode and typically platinum metal as a cathode (Fig. 1). The cell is filled with an electrolyte containing hydrofluoric acid (HF). High anodic currents produce smooth silicon surfaces in a process called electropolishing. With lower anodic currents pores are etched on the surface of the silicon producing a porous film.

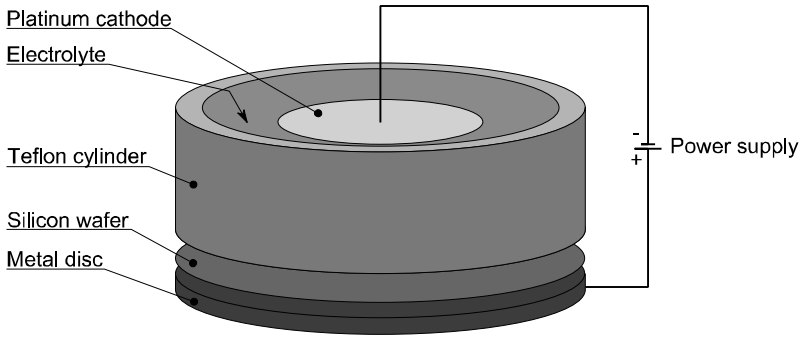

Figure 1. *Electrochemical cell used to produce porous silicon.*

The formation mechanisms of PSi involved in the electrochemical etching are very complex and are currently not completely understood [19]. A simplified description of pore formation can be made by considering the three processes independently: dissolution of a silicon atom, pore initiation and pore growth.

No significant dissolution of Si surface takes place in acidic HF solutions in the absence of holes (empty electron state in the valence band) in Si [22]. The otherwise reactive Si surface is kinetically stabilized by the hydrogen termination of the surface formed in HF solutions.

However, in the presence of holes, the dissolution of silicon atoms can take place at the surface [22]. Holes are usually generated either by an anodic bias or by illumination.

Illumination is used especially with n-type silicon in which the holes are the minority charge carriers. The anodic bias causes the holes to drift to the Si-electrolyte interface. A hole weakens the Si-Si bond of a surface atom and the atom is dissolved by HF following the overall reaction which takes place in the most commonly studied conditions [22]:

$$\mathrm{Si} + 6\mathrm{HF} + \mathrm{h}^{+} \rightarrow \mathrm{SiF}_6^{-2} + 4\mathrm{H}^{+} + \mathrm{H}_2 + \mathrm{e}^{-}. \qquad (2.1)$$

In order for the surface to become porous, the etching must take place selectively on the surface. If all the surface atoms have an equal probability to dissolve, the surface would only roughen and thus no pore formation would take place. It has been postulated that certain features of the interface make some silicon atoms more likely to dissolve than others, initiating the pore growth. These features include structural defects, mechanically strained areas or local perturbations in the surface potential field [19].

Once pores have been initiated, there must be a certain mechanism (or mechanisms) to induce the etching to take place preferably at the pore tips instead of the pore walls. Mechanisms relying on either chemical properties of silicon or physical mechanisms have been proposed [23]. The chemical mechanisms propose that the local environment at the pore tips makes the silicon atoms more reactive towards dissolution [23]. Some of the physical mechanisms involve a thinning of the depletion layer. The depletion layer is a layer at the semiconductor interface which is depleted from charge carriers. The thinning of the depletion layer in the vicinity of the pore tips makes it easier for the holes to reach the surface atoms at the pore tips as compared to the pore walls [23]. In addition, passivation of the pore walls is also proposed to be due to the depletion layer [24] or quantum confinement arising from the narrow thickness of the pore walls [25]. Quantum confinement effect causes an energy barrier for holes, consequently reducing their probability to drift into the pore walls.

At present, there is no single all-encompassing "unified theory of etching". Indeed, its formulation would be a formidable challenge because of the wide variety of PSi

structures that can be created under various conditions. The structures can vary from microporous to macroporous, as well as those with highly regular pores to pores with branched (Fig. **2**) and sponge-like structures. The porosity can be anywhere between 5 % and 95 % and surface area can range between 10 and 1000 m^2/cm^3 [19].

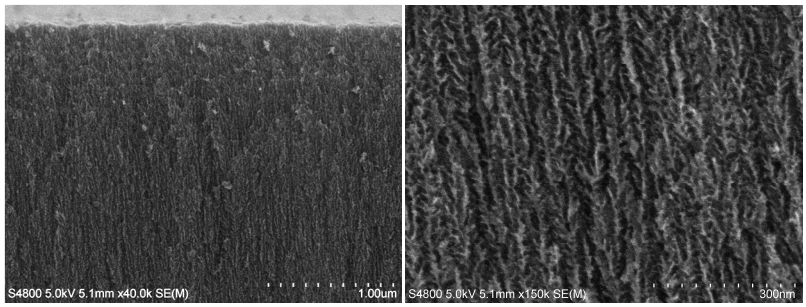

Figure 2. *Scanning electron microscopy images of a cross-section of PSi. Pores are aligned vertically and exhibit a branched structure.*

There are numerous fabrication parameters affecting the structure of PSi including the type and concentration of dopants in silicon, crystallographic orientation of Si, composition of electrolyte, illumination, current density, stirring of the electrolyte and temperature [19]. Because of the high number of parameters, their complex interdependency and lack of theoretical understanding, the effect of different fabrication parameters on the structure is mainly understood on an experimental basis.

The structure of PSi can also be modified after the etching. The annealing of PSi at a high temperature in an inert atmosphere causes coarsening of the structure [26]. The driving force for the process is the minimization of surface energy and consequently of surface area as smaller pores become fused together, forming larger pores [27]. The process becomes kinetically possible at high temperatures because of the increased mobility of Si atoms. The increased mobility is not only due to the increased kinetic energy of the atoms but also because of the changes in the surface chemistry. Surface hydrides desorb at temperatures between 260 °C and 500 °C

causing a reorganization of the surface and creation of dangling bonds (unpaired electrons) which make possible the structural changes [28]. The first signs of changes in the crystal structure of PSi are observed at 350 °C but significant changes in the pore structure take place at a temperature of 500 °C or higher when most of the hydrogen has desorbed [28, 29]. It should be mentioned that the structural changes taking place during annealing occur in hydrogen terminated PSi, whereas oxidation of the surface stabilizes the structure against coarsening [26].

In addition to the pore structure, another very important feature of PSi, as of any other mesoporous material, is its surface chemistry. The native surface of PSi after etching is hydrogen terminated [30]. Mono-, di-, and trihydride species form a dense layer at the surface. As mentioned earlier, the hydrogen termination provides a passivating layer on the otherwise highly reactive silicon. However, the passivation is not complete, instead the hydrogen terminated PSi undergoes a slow oxidation with oxygen or water molecules even under ambient conditions [31]. In addition, hydride groups can act as reducing agents for example with drug molecules loaded in the pores [32]. Therefore, it is important to stabilize the surface in order to produce a material with properties that do not change as a function of time, and also a material that does not cause undesirable changes to the guest molecules in the pores.

PSi is mainly stabilized via the addition of either oxygen or carbon atoms in the structure. Both Si–O and Si-C bonds are stronger and more stable than either Si–Si or Si–H bonds [33]. Therefore, a silicon oxide or silicon carbide layer on the pore surface will efficiently stabilize the structure.

Oxidation of PSi is typically performed by thermal oxidation or liquid phase oxidation. In thermal oxidation, PSi is heated in an oxygen-containing atmosphere. Rapid oxidation begins at 250 °C with backbond oxidation of the Si–Si bonds of the surface atoms [34, 35]. The surface hydrides are oxidized into Si–OH groups at a slightly higher temperature because of the higher bond strength of Si–H compared with Si–Si [35]. At a sufficiently

high temperature, 800 °C and above, complete oxidation of the PSi structure into SiO_2 is possible [36].

Another frequently utilized oxidation method is a liquid phase oxidation with chemical oxidants such as H_2O_2 and HNO_3 [37-39]. Furthermore, oxidation can be performed by removing, at least partially, the stabilizing surface hydrides by annealing and subsequently exposing the material to air, which causes a rapid oxidation of the surface [40].

Oxidation not only affects the surface chemistry, but it also affects the pore structure of PSi. In the oxidation process, an oxygen atom is added between two silicon atoms, causing a volume expansion of the material. Therefore, decreased pore volume and pore size have been observed after oxidation [41]. However, the effect of the oxidation on the pore size has not been widely studied.

Stabilizing the PSi surfaces with carbon can lead to even more stable structure than oxidation. Although the bond strength of Si–C is lower than that of Si–O, it is more stable because of the lower polarity of the bond, making it less susceptible to nucleophilic attacks [30].

One beneficial method of generating highly stable Si-C surfaces on PSi is thermal carbonization [42, 43]. This technique is carried out by thermal decomposition of acetylene (HC≡CH) on a hydrogen terminated surface. At temperatures below 600 °C, a hydrophobic hydrocarbon surface is produced by desorption of hydrides and dissociation of acetylene on the surface. The product is referred to as thermally hydrocarbonized PSi (THCPSi). At temperatures above 600 °C, the carbon from acetylene penetrates into the structure of PSi forming a nonstoichiometric silicon carbide layer on the surface. The hydrophilic material produced is referred to as thermally carbonized PSi (TCPSi).

2.1.2 Ordered mesoporous silica

The early history of another important type of mesoporous materials, ordered mesoporous silicas, is curiously similar to that of PSi. The first record of this type of materials can be found

in a patent about the production of low density silica filed in 1969 [44]. Unfortunately, it was not known at the time that the product was an ordered mesoporous silica, this fact was only confirmed decades later [45]. These types of materials were (re)discovered 20 years later in 1990 [46]. A highly influential report of an ordered mesoporous silica MCM-41 (Mobil crystalline material) was published by a group of scientists from Mobil Research and Development Corporation in 1992 [47]. This report sparked a wide interest in this type of materials, around the same time that the research in PSi was rapidly increasing. A further advance in development of the ordered mesoporous silicas was the discovery of SBA-15 (Santa Barbara Amorphous), which had a larger pore size, thicker pore walls and improved hydrothermal stability [48].

The production of ordered mesoporous silicas differs fundamentally from that of PSi. Whereas PSi is a so-called top-down material in which the mesostructure is etched into bulk silicon, the silicas are bottom-up materials, i.e., molecules are assembled to form the mesostructure. The assembly is achieved by using surfactant micelles as the template on which silica is condensed [48].

A surfactant (i.e. surface active agent) is a substance that has a tendency to adsorb onto surfaces and interfaces and significantly alters the surface or interfacial free energy. These substances are typically molecules with hydrophobic and hydrophilic parts. In aqueous solutions of surfactants, free energy is lowered when the hydrophobic parts of the molecules pack together to minimize their interaction with water [49]. On the other hand, the hydrophilic parts interact favorably with water and form a layer surrounding the hydrophobic core. The formed aggregates can have different shapes e.g. spherical or rod-like micelles, or lamellar structures depending on the structure of the surfactant and the properties of the solution such as concentration and temperature [49].

In order to synthesize SBA-15, micelles of amphiphilic triblock copolymers are used as templates on which silica is polymerized to form the pore walls [48]. The copolymer is linear

containing hydrophilic poly(ethylene oxide) end sections and a hydrophobic poly(propylene oxide) middle section. The formation of the SBA-15 structure has been observed to take place via two distinct pathways. In the first pathway [50, 51], the surfactant forms spherical micelles in the solution. Silica is adsorbed and polymerized onto the surface of the micelles and the spherical micelles form flocks. The micelles then start fusing together forming rod-like structures, which eventually create the hexagonally packed structure. In the second pathway [52], surfactant also forms spherical micelles in the solution. The spherical micelles become fused into rod-like micelles when silica starts to adsorb and polymerize onto them. The rod-like micelles form bundles and subsequently the bundles create a hexagonal structure. After the formation of the hexagonal structure, the surfactant is extracted by chemical dissolution or by calcination at a high temperature [48].

The mechanism of the synthesis of MCM-41 is similar to that of SBA-15, although there are also significant differences [47]. The key difference is that instead of the amphiphilic triblock copolymers, smaller cationic surfactants are used as templates. Thus, smaller pores are formed because of the smaller size of template molecules. Because of the different template molecules, the interaction between the surfactant micelles and silica precursor differs in the synthesis of MCM-41 compared to the synthesis of SBA-15. The interaction is electrostatic in its nature in the MCM-41 synthesis whereas in the synthesis of SBA-15, the interaction is believed to be due to electrostatic forces, hydrogen bonding and hydrophobic attraction [50, 53]. Furthermore, synthesis conditions are different for the two materials. For example, while SBA-15 is synthesized under acidic conditions, MCM-41 is synthesized under basic conditions [54].

SBA-15 has a well ordered structure of cylindrical pores packed together in a 2D hexagonal structure (Fig. 3). The mesopore size distribution is very narrow and the pore size can be tuned in the range of 6 nm to 15 nm by changing the size of the template polymer and altering the synthesis conditions [55]. In addition to the mesopores, the pore walls of the material

contain micropores which are formed by polymer chains embedded in the silica during the synthesis [56]. Another interesting feature of SBA-15 is the presence of u-shaped pores within the structure [57].

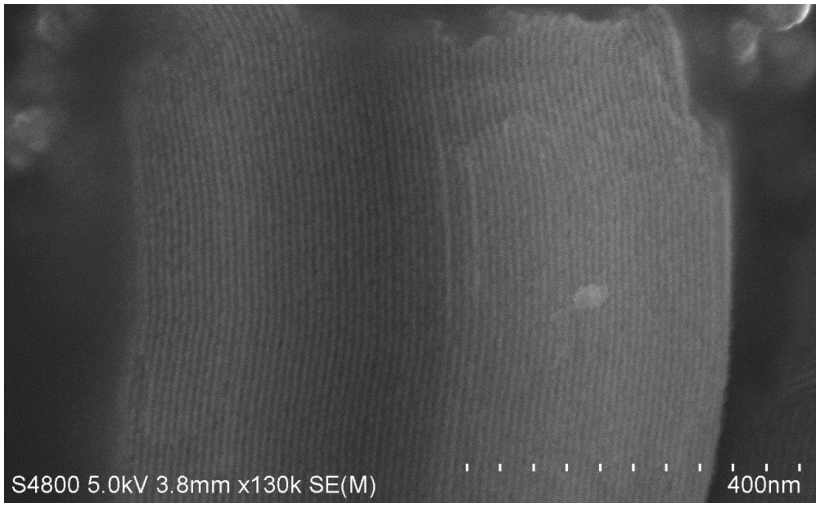

Figure 3. *Scanning electron microscopy image of SBA-15 showing its pore structure.*

The pore walls of SBA-15 consist of amorphous silica and the pore surface contains a high density of Si-OH and Si-$(OH)_2$ species [53]. In addition to purely siliceous SBA-15, an aluminum containing SBA-15 (al-SBA-15) can be prepared via the addition of aluminum during synthesis [58].

2.2 CHARACTERIZATION OF MESOPOROUS MATERIALS

For successful development of mesoporous drug delivery systems, thorough knowledge of their properties is essential. The main properties to be characterized are pore structure (pore size, pore volume surface area and pore morphology) and surface chemistry. These properties have a major impact on the behavior and applicability of the drug delivery system. For example, the pore structure will affect the loading capacity of a carrier and the release of drugs from the pores. Furthermore, surface chemistry can affect e.g. loading of drugs and the

chemical compatibility between the carrier and the drug molecules.

2.2.1 Pore structure

Electron microscopy is often used to examine the nanoscale structure of mesoporous materials. Scanning electron microscopy (SEM) is based on scanning a sample with a narrow electron beam and recording the intensity of scattered electrons at each point on the surface. This produces images of surfaces with a three-dimensional appearance, making it possible to visualize the surface structure, with resolution reaching 1 nm. Transmission electron microscopy (TEM) reveals the internal structure of materials by directing an electron beam through a thin sample and then focusing a magnified image of the sample on a fluorescent screen. The contrast of the images reflects absorption of electrons in the sample. TEM makes it possible to image fine details of materials thanks to a high resolution which can reach atomic length scale. In this context, the greatest advantage of these methods is their versatile ability to determine pore morphology [59]. For example, the shape of the pore cross-section and the pore walls as well as regularity of the pore stacking can be observed. However, it can be very laborious to obtain statistically significant values of the pore diameter.

Gas sorption is probably the most common method to measure the properties of the pore structure [60]. The basis of the method lies in observation of a gas-liquid phase transition in pores. In practice, an adsorption or desorption isotherm is recorded by measuring the volume of a condensed gas as a function of pressure under isothermal conditions. According to the Kelvin equation, the condensation pressure is dependent on the curvature of the liquid-gas interface and the curvature is dependent on the diameter of the pore where the interface is located. The BJH (Barrett Joyner Halenda) theory [61] is often used to convert a recorded isotherm into a pore size distribution. The pore sizes that can be measured with gas sorption methods are between 0.5 – 200 nm [62]. An important

advantage of the gas sorption methods is that, in addition to the pore size and pore volume, surface area can be independently calculated usually by BET (Brunauer Emmet Teller) theory [63] which is based on observation of the multilayer adsorption of gas on surfaces. In addition to the quantitative analysis, also qualitative information can be obtained about the pore morphology. Features in the pore morphology cause characteristic features in the adsorption and desorption isotherms. An example of such a feature is an ink-bottle pore (Fig. 4), in which a larger pore is connected to the exterior of the particle by smaller pores (bottle necks) [64].

Thermoporometry is an interesting, although much less used, method for characterizing mesoporous structures [65, 66]. In thermoporometry, the liquid-solid transition in the pores is observed and thus differs from gas sorption where the gas-liquid transition is observed. Since freezing or melting temperature inside a pore is dependent on its diameter, the diameter can be calculated by measuring freezing or melting of a substance in the pore. Furthermore, pore volume can be calculated from the measured melting enthalpy of a substance in the pores. Therefore, pore size distribution can be calculated from a heat flow curve measured by differential scanning calorimeter (DSC) over the temperature range of melting or freezing. The pore sizes that can be measured by this technique are typically in the mesopore range. However, up to 300 nm pores have been measured [67]. In order to obtain a better understanding of the method and results presented later, some confinement effects on properties of materials in mesopores are discussed below.

Thermoporometry is based on the melting point depression of confined materials [68]. When loaded in the pores, an adsorbate is divided into numerous small individual parts i.e. the adsorbate in a single individual pore forms its own "particle". Since the size of these particles is very small, they have a large surface area to volume ratio A/V and this ratio has an important impact on the melting temperature. The melting temperature can be determined by the free energy of the system.

It can be divided into a surface and volume contributions in which surface contribution favors liquid state and volume contribution favors solid state. The surface contribution to the free energy of the system becomes significant with high A/V values of the particles in the mesopores and melting point is shifted to lower values as compared to large particles [69]. In analytical treatments, it is practical to use the surface curvature $\kappa = dA/dV$ instead of the area-to-volume ratio. An equation which relates the curvature to the melting point depression ΔT is the Gibbs-Thomson equation: $\Delta T = -K\kappa$, where K is often assumed to be a constant. As a result, by assuming the shape of the liquid-solid interface during phase transition, the pore size can be calculated from the Gibbs-Thomson equation [68].

Typically, melting and freezing in the pores takes place at different temperatures. By measuring this melting-freezing hysteresis phenomenon one can gather information about the pore morphology. The reasons for this hysteresis have been discussed in the literature [68, 70, 71]. In their highly influential article, Brun et al. suggested that the reason for the hysteresis is the difference in the shape of the solid-liquid interface during melting and freezing [68]. In the presence of a bulk solid phase at the pore openings, freezing is nucleated from a bulk phase and propagates via a hemispherical solid-liquid interface. In contrast, during melting, the solid-liquid interface follows the shape of the pores. Therefore, the curvature of the interface is almost always smaller during melting than freezing, leading to this hysteresis behavior.

Another reason for melting-freezing hysteresis is a presence of ink-bottle shaped pores (Fig. 4) [71]. Smaller adjacent segments (bottlenecks) can cause supercooling in a wider segment of the pore. The reason behind this effect is that the freezing in a certain segment of a pore must be heterogeneously nucleated from previously frozen adjacent segments. If a nucleation center is not present at an adjacent narrower segment, the material in the wider segment cannot freeze, even though this would be thermodynamically possible. Heterogeneous nucleation is required since homogeneous

nucleation in the pore is highly unlikely because of the small dimension of the pore. Exceptions to this phenomenon are temperatures at and below the homogeneous nucleation temperature, at which the nucleation rate becomes high enough for homogeneous nucleation to become significant. On the other hand, melting can take place individually in each segment without nucleation and, therefore, any solid in the pores does not become superheated.

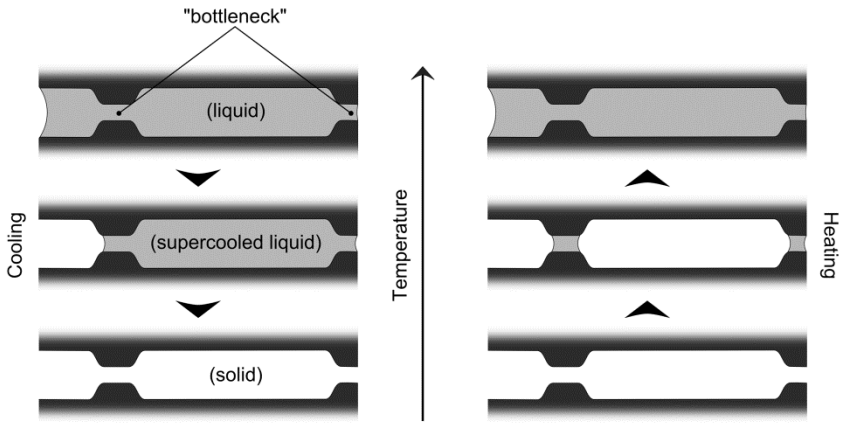

Figure 4. *Freezing and melting in an ink-bottle pore. Freezing is delayed by the bottle necks causing supercooling in the wider parts of the pore.*

A striking feature of solids confined in pores is that the whole volume of the pore is not occupied by the solid phase [65]. Instead, a thin liquid-like layer exists between the pore wall and the solid core. This is called the δ-layer and it exists because it is energetically more favorable for a liquid rather than for a solid to wet the pore wall [72]. The thickness of the delta layer (δ) is mainly dependent on the interactions existing between confined molecules and the pore wall [73]. The δ-layer is typically two to three molecule layers thick and can therefore occupy a significant part of the pore volume within a narrow pore [65].

When using thermoporometry to determine pore sizes, it is important to take into account the δ-layer. Since the radius that is calculated by the Gibbs-Thomson equation (R_c) is the radius of the crystal inside the pore and the pore radius (R_p) is

determined by the following equation $R_p = R_c + \delta$. The thickness of the δ-layer is often calculated using experimentally determined volume of the crystalline part of the adsorbate and the total volume of adsorbate and an assumed pore geometry.

X-ray diffraction (XRD) can also be used to measure structure of porous materials. Since XRD provides information about long range ordering of a material, a different type of information is obtained when investigating ordered mesoporous silicas and PSi. In ordered mesoporous silicas, atoms in the pore walls exist in a disordered state. On the other hand, the pores exhibit long range ordering. In accordance with Babinet's principle, diffracted radiation from a porous material is identical in intensity but opposite in phase to "an inverse material" in which the material and empty space are inverted in comparison with the porous material. Therefore, the diffraction pattern of SBA-15 is similar to the diffraction pattern of hexagonally ordered rods. The pattern contains information about the distance between adjacent pores, arrangement of the pores and the quality of the long range order. For example, the 2D hexagonal ordering of SBA-15 can be confirmed by indexing the diffraction peaks in the diffractograms. At least three diffraction peaks (from planes [100], [110] and [200]) should be observed at low Bragg-angles [53].

In contrast to the situation with ordered mesoporous silica, PSi does not typically exhibit ordering of the pores but the atoms in the pore walls are ordered in a crystalline structure. Therefore, the information obtained from PSi is related to the properties of the crystal e.g. distances between atoms and crystallite size. A typical diffraction peak of PSi consists of a sharp peak superimposed on a wide diffuse scattering [74]. The sharp peak arises from the long range crystalline ordering of the material. The origin of the diffuse scattering is more controversial. According to Buttard et al., this is due to small crystals, i.e. crystallites, present in the material and the width of the diffraction peak reflects the crystallite size [75]. However, Bensaid et al. argued that it arises from the pores following Babinet's principle [74]. According to this explanation, the width

of a diffraction peak reflects the size of the regions lacking the crystal structure, i.e. the pores and possible noncrystalline surface layer.

2.2.2 Surface chemistry

Spectroscopic methods have been widely used to characterize the surface chemistry of mesoporous materials. Probably the most popular spectroscopic method in this context is Fourier Transformation Infrared Spectroscopy (FTIR). This technique can be used to measure absorption of electromagnetic radiation in a sample as a function of a wavenumber, using an interferometer. The absorption spectrum in the mid-infrared region is especially useful since the spectrum contains information about chemical bonds commonly found at the surface of mesoporous silicon and silica, such as O-H, Si-H and Si-O [76]. Each chemical bond can vibrate at certain characteristic frequencies, and in most cases, there is a change in the dipole moment of the bond related to the vibration. The bonds only absorb photons with characteristic energies (and thus wavenumbers) that exactly match the energy difference between vibrational states of a molecule. These photons are able to excite the molecule to a higher energy state and are consequently absorbed.

Various other spectroscopic methods have also been applied in the characterization of mesoporous materials. These include Raman spectroscopy, which provides similar information as FTIR, and nuclear magnetic resonance spectroscopy (NMR) which can be used to characterize the chemical environment of atoms [77, 78].

2.3 DRUG DELIVERY WITH MESOPOROUS MATERIALS

An improvement of dissolution of poorly soluble drugs by loading into porous material was already reported in 1972 [79]. In that report, drugs were adsorbed onto the surface of fumed silica. Fumed silica consists of small aggregated particles giving

rise to a large surface area and interparticle porosity. Considerable scientific interest in mesoporous materials as drug carriers was triggered in 2001 when Maria Vallet-Regi proposed that MCM-41 could be used as a drug delivery vehicle to achieve the sustained release of drugs [80]. The field has since broadened to include improved release of poorly soluble drugs [81], targeted cancer treatment [82] and gene delivery [83]. These are only some of the new possibilities proposed for the nanostructured materials during last decade.

2.3.1 Loading

Several therapeutically active small molecules have been loaded into mesoporous materials [11, 81]. Poorly soluble drugs are popular in these types of studies because their dissolution can be readily enhanced by mesoporous carriers. In addition to small molecules, peptides and proteins have been loaded into mesopores in order to obtain a sustained release [84, 85].

Drug loading into mesoporous materials is commonly carried out with solvents by either immersion or impregnation methods [86, 87]. These methods are able to produce high drug loads at room temperature.

In the immersion method, the carrier is immersed in an excess of drug solution and drug is adsorbed onto the surfaces. In addition to the adsorbed drug, some drug molecules exist in a dissolved state in the pores. After the adsorption, the carrier is filtered out of the solution and dried. It is relatively easy to prevent extensive deposition of the drug on the external surface of the carrier in this method by reducing the drug concentration in the loading solution. However, the lack of precise control of the drug load and drug wasted in the filtration step are viewed as disadvantages of this method [86, 87].

The impregnation method begins by of addition of a drug solution onto a carrier followed by evaporation of the solvent which drives the drug molecules into the pores by diffusion [86, 87]. The term incipient wetness impregnation refers to a method where the volume of the solution equals the pore volume [88]. A true incipient wetness method results in rather low drug

contents and is therefore not commonly used, although the term is loosely applied for all impregnation methods [87]. The main benefit of the impregnation method is the low amount of wasted drug and the good control over the loading degree. However, the presence of drug deposited outside the pores can be problematic because the benefits of using the mesoporous carrier are realized only for the portion of drug that is located inside the pores [86, 89]. Drug on the external surface of particles is especially disadvantageous for delivery of poorly soluble drugs because the slowly dissolving drug on the external surface prevents access of the release medium to the pores.

2.3.2 Characterization of loaded mesoporous carriers

The following aspects of drug loaded mesoporous carriers need to be characterized in order to understand their behavior; amount of loaded drug (loading degree), chemical state, physical state and the release profile of the drug.

The amount of drug in the carrier is usually determined by thermogravimetry (TG) or by dissolving the drug in a solvent and analyzing the drug concentration of the solution, e.g., by high performance liquid chromatography (HPLC) or ultraviolet-visible spectroscopy (UV/VIS) [81]. TG analysis is based on the differences in the thermal degradation temperatures of the carrier (typically inorganic) and the drug (organic). By heating the sample above the drug degradation temperature while recording the weight of the sample, the drug loading degree can be calculated.

Because of the high pore volume and surface areas, high drug loads in the materials can be achieved and drug loading degrees up to 60 % have been reported [89]. The drug loading degree is defined here as the mass of drug in the carrier divided by the total mass of the loaded carrier.

It is important to characterize the chemical state of the drug in order to determine whether degradation has taken place in the drug carrier. Drug degradation is typically evaluated by dissolving the loaded drug and analyzing the solution with

HPLC [90]. Many studies, that assessed the chemical integrity of the loaded molecules, reported the drug to remain chemically intact [11, 91]. However, more problematic drug–mesoporous carrier combinations, resulting in chemical instability of the drug, have also been described [11, 90, 92].

The chemical state of drugs is also characterized in order to assess if the drug has chemisorbed on the pore walls, i.e., whether a chemical bond has formed between the pore wall and the drug molecule. Chemisorption of a guest molecule on a carrier surface can be determined by adsorption-desorption experiments where chemisorption is revealed by the irreversible adsorption of the molecule on the surface [93]. It is also possible to determine chemisorption spectroscopically by observing if changes in chemical bonds have occurred during adsorption [94].

The physical characterization of the drug loaded carriers provides information about ordering of the drug (crystalline/amorphous) and its location in the carrier. The drug can exist in four distinct forms: crystalline outside the pores, nanocrystalline inside the pores, amorphous or sparsely dispersed on the pore walls. The amorphous form in the pores can be present as a δ-layer between the crystal and the pore wall or as the only phase in the pores.

Since the pore structure restricts the size of any crystals in the pores, any large crystals found on the sample must be located outside the pores [95]. The size of the crystals in the pores can be detected with DSC because of the above mentioned size dependent depression of the melting temperature. Therefore, melting of drug detected at the bulk melting temperature is evidence of drug crystals outside the pores and melting at lower temperatures points to a nanocrystalline phase inside the pores.

If the drug is not in a crystalline state, a glass transition should be detected with DSC provided that the drug is forming amorphous clusters in or outside the pores [87]. In addition, the glass transition temperature may change if an amorphous material is confined within the pores [96]. On the other hand, the absence of melting and glass transition implies that the drug

is deposited on the pore surfaces without formation of larger clusters [87].

Some information about the location of the drug can also be obtained by measuring the pore size and pore volume of drug carrier with gas sorption before and after loading [87]. A reduction of the pore size points to a formation of a drug layer on the surface of the pores. If the pore size is not affected, but the pore volume is decreased, then the pores are partially blocked by the drug but an adsorbed layer has not formed on the pore walls. If there is no porosity detected after loading, then pores are most probably blocked by the drug.

In most of the reports, especially with mesoporous silica SBA-15 and MCM-14, loaded drugs have been detected in a disordered form inside the pores [11, 87, 89, 97]. Although an amorphous phase is thermodynamically unstable as compared to its crystalline counterpart in bulk, the stability of a disordered phase in mesopores is usually found to be good since no crystallization has been observed even in humid atmospheres after storage of several months [11, 98, 99]. The crystal growth is prevented by the small dimensions of the pores where the drug is located. A crystal nucleus has to reach a certain critical size in order for crystal growth to be energetically favorable [100]. If the pore size is smaller than this critical size, the crystals cannot form inside the pores and the amorphous phase is stabilized. However, in larger pores with a diameter above 10 nm, there are also reports of the presence of drug in the crystalline phase [95, 101].

Mellaerts et al. reported that the loading method influenced the location of the drug in mesoporous materials [87]. Impregnation of SBA-15 with a concentrated itraconazole solvent resulted in molecularly dispersed drug on the pore walls. On the other hand, impregnation with a dilute itraconazole solution resulted in the formation of amorphous clusters of the drug in the pores. Independent of the concentration of the solution, ibuprofen was molecularly dispersed on the pore walls.

The surface chemistry of mesoporous materials has been found to affect the structure and biological activity of adsorbed proteins [102]. This result highlights the importance of compatibility between the guest molecule – pore surface and the determination of biological activity of the loaded molecules.

2.3.3 Drug release from mesoporous carriers

The principle of measuring an *in vitro* release profile of drugs from carriers is simple. Drug loaded carriers, often in a powder form, are immersed in a release medium and the concentration of the drug in the medium is measured as a function of time. There is a wide variety of different methods available with which to evaluate the dissolution process [103]. These methods can vary depending on the type of release medium and its volume, and the technique and rate of stirring. The concentration of the drug in the release medium can be measured by taking small samples or it can be assayed continuously in the dissolution vessel. It is important to separate the solid materials from the release medium when measuring the dissolved concentration [103]. This can be achieved by membranes, sedimentation or centrifugation.

It should be noted that the above mentioned simple *in vitro* dissolution methods often do not correlate well with the *in vivo* release. The system is very complex in the *in vivo* environment because of the numerous chemical substances present, the varying mechanical stimulus and the interactions between the carrier and living cells. Therefore, simple *in vitro* release experiments are more useful for determining properties of the delivery system rather than assessing its behavior in the final application *in vivo*.

Numerous combinations of potential drug carriers and poorly soluble drugs have been tested in release experiments [11, 81, 104]. The release rate of the drugs has been consistently found to be improved significantly as compared with the dissolution rate of the pure drug. For example, 75 % of furosemide loaded into PSi was released within 60 min compared to only 5 % from pure crystalline drug. It has also

been demonstrated that release of poorly soluble drugs from mesoporous carriers can produce supersaturated concentrations in the release medium [105].

The improvement in the release behavior is attributed to the disordered or the nanocrystalline state of the drug or to the large surface area in from which the drug can be dissolved [10, 101]. As stated earlier, the drug is often present in a disordered state in the pores. Since a disordered material is at a higher energy state compared to a crystalline form, the apparent solubility is significantly increased [106]. The apparent solubility will also be increased if crystals are formed in the pores because of the small size and consequently the large curvature of the crystals [107]. The high apparent solubility leads to higher dissolution rates [108]. On the other hand, the high surface area in contact with release medium also increases the dissolution rate. A high surface area is achieved when the drug is located on the pore walls, leaving free the center of the pore.

It should be noted that apparent solubility refers to the saturation concentration that can be formed by dissolution of a solid that is not in its most stable form [109]. This should not be confused with equilibrium solubility i.e. a true thermodynamic solubility, which is the concentration of a substance in a solution in equilibrium with the most stable solid form. The apparent solubility of a drug depends on the solid form of the drug but this is not the case for the equilibrium solubility.

In peptide/protein delivery, a sustained release is preferred because of the short duration of activity of these compounds [7, 9]. Sustained release can be achieved with mesoporous carriers [110, 111], even though it might be difficult to appreciate why that the same carrier can be used to enhance the release for some compounds but also to delay the release of other compounds. The sustained release from mesoporous carriers is attributed to the relatively strong adsorption of the molecules onto the pore surfaces and their slow diffusion in the narrow pores [110]. Because of the high surface area of the mesoporous carriers, there may be a high number of molecules in direct contact with the pore surface. The attachment can be due to hydrogen

bonding, electrostatic attraction, van der Waals forces or hydrophobic interactions. Covalent bonding can also be utilized, but it must be carefully designed in order to ensure that the structure of the released molecule remains functional. The sustained release of proteins and peptides is also facilitated by the properties of these molecules. They tend to be "sticky" because they can have regions with divergent properties such as hydrophobic, hydrophilic areas and positively and negatively charged parts etc. [112]. Furthermore, these molecules can adopt different conformations to accommodate to the features of the surfaces [112].

Several parameters affect *in vitro* release rate of drugs from the mesoporous carriers. Strong surface – drug interactions are known to reduce the release rate [113, 114]. A well known example is delayed release of ibuprofen from a carrier modified with amino groups as a consequence of a coulombic attraction between protonated amino groups on the surface and deprotonated carboxylic acid group of ibuprofen [115, 116].

The pore structure has also an important effect on the release. A decrease in pore diameter has been found to reduce the release rate in pores under 13 nm in diameter. [89, 117]. This effect is attributed to diffusion restrictions or purely to drug - surface interactions [89, 118]. Although a large pore size can facilitate fast release from the carrier, it can also promote crystallization of a drug in the pores. The presence of drug crystals in pores has been found to decrease the release rate as compared with the amorphous state [101]. If crystalline material is present on the surface of the pores, it can have a decelerating effect on the release rate, especially with poorly soluble drugs [10]. Furthermore, pore shape and interconnectedness have been reported to affect the release rate. For example, small pore openings hindered the release whereas interconnectedness of the pores facilitated the release [104, 117].

A sustained release can be achieved by compressing mesoporous powders into tablets [80, 117]. The compression of particles with diameters in the range of microns into tablets with

dimensions in millimeters significantly delayed the diffusion of the guest molecules from the structure.

Although *in vitro* dissolution testing can be useful in assessments of the drug carriers, more relevant results can be obtained by *in vivo* testing. Despite numerous promising *in vitro* studies, there are still relatively few reports of *in vivo* delivery of poorly soluble drugs with mesoporous carriers [87, 91, 97, 119-123]. In these studies, the bioavailability of a drug has been assessed by measuring the drug concentration in plasma after oral administration. Improved bioavailability compared with pure drug has been observed in all of these published studies. In comparison with commercial formulations used to enhance bioavailability, improved or a comparable bioavailability has usually been reported with mesoporous carriers. As much as a fourfold increase has been observed in bioavailability with a mesoporous carrier as compared with a commercial formulation [121].

In addition to oral administration, mesoporous drug carriers have been used to deliver various therapeutic agents via parenteral routes [124, 125]. There is considerable interest in using these carriers in cancer therapy [124, 126].

A beneficial way to evaluate a performance of a drug formulation is to measure a physiological response to the drug after its administration. This is especially important when the administered drug is a peptide or a protein since these compounds can easily lose their bioactivity through degradation or after changes in their three-dimensional folding. Recently, the physiological response to a few peptides released from PSi has been studied, demonstrating that they achieved a sustained physiological effect [127, 128].

3 Aims of the study

Preclinical development of mesoporous materials as drug delivery systems includes the production of carriers, the characterization of unloaded and loaded carriers, and the evaluation of drug release from these structures. In the present work, all four aspects have been studied. The specific aims of the study were:

1. To develop a method to achieve the controlled enlargement of pores in PSi by thermal annealing.
2. To assess the effects of various oxidation methods on structure and surface chemistry of PSi and to develop oxidation methods for producing inert surfaces on PSi with minimal changes in the pore structure.
3. To develop a method for quantifying the amount of u-shaped pores in SBA-15.
4. To provide detailed knowledge of the physical state of a drug in the pores of PSi with various surface chemistries and different pore sizes.
5. To determine whether PSi could be used as a carrier to achieve sustained release of a peptide.

4 Experimental

An overview of materials and experimental procedures used in the present work is presented here. A more detailed description can be found in the original publications.

4.1 MATERIALS

PSi was produced from boron doped Si wafers with resistivity of 0.015 Ωcm – 0.025 Ωcm (I and V) and 0.01 – 0.02 Ωcm (II and IV). The wafers were 100 mm in diameter and the etched surface was oriented along the crystallographic plane (100). The electrolyte used in etching was a mixture of ethanol (99.5 %) and HF (37 %–39 %) with ratios 2:3 (I), 1:1 (I, II and V) and 4:5 (IV).

MCM-41 was produced with cetyltrimethylammonium bromide as the structure directing template, and fumed silica, tetramethyl ammonium silicate and sodium silicate as the silica sources.

SBA-15 was produced with Pluronic P123 triblock copolymer as the structure directing template and tetraethyl orthosilicate as the silica precursor in the presence of hydrochloric acid. In the aluminum containing Al-SBA-15, aluminum isopropoxide was used as the source of aluminum.

Two poorly soluble drugs, cinnarizine (II) and ibuprofen (IV) and a peptide ghrelin antagonist (GhA, [D-lys-3]-GHRP-6) (V) were used as model compounds. Cinnarizine is an antihistamine and ibuprofen an anti-inflammatory drug. GhA blocks ghrelin receptors and causes a reduction in the food intake and an elevation in blood pressure. It is a relatively small (930 g/mol) peptide consisting of six amino acids (H-His-D-Trp-D-Lys-Trp-D-Phe-Lys-NH2).

4.2 METHODS

4.2.1 Porous silicon

All PSi was prepared by electrochemical etching in a type of cell presented in Fig. 1 with current densities of 20 mA/cm^2 (I and IV) and 50 mA/cm^2 (I, II, IV and V). A high current pulse was applied at the end of the etching to dissolve the silicon between the porous film and the silicon wafer in order to make it easier to remove the porous film. The porous film was dried at 65 °C and subsequently ball milled to produce PSi microparticles. In article II, both free-standing films and microparticles were used. After milling, the PSi powder was sieved into separate desired particle size fractions. Since milling causes oxidation of PSi surface, the powder was treated with a 1:1 mixture of HF and ethanol to replace the oxide surface with hydrogen termination.

Annealing was carried out with hydrogen terminated particles in a quartz tube in a tube oven (I, II and IV). A continuous nitrogen flow of 1 l/min was applied while the sample was heated to temperatures between 400 °C and 1000 °C. In this study, annealing is defined as heating in an inert atmosphere (nitrogen gas), not to be confused with thermal oxidation in which the sample is heated in air.

Surface stabilization was performed to PSi by oxidation, thermal hydrocarbonization or thermal carbonization. Thermal oxidation was performed by heating the PSi at 300 °C for 2 h (IV). In article II, several oxidation methods were performed, varying from thermal oxidation to liquid phase oxidation and high temperature annealing followed by exposure to ambient air.

Thermal hydrocarbonization was performed by continuous flushing with a 1:1 mixture of acetylene and nitrogen gases (2 l/min) at 500 °C for 15 min. In thermal carbonization, the first step was identical to thermal hydrocarbonization and in the second step, the sample was flushed with the 1:1 mixture of acetylene and nitrogen at room temperature followed by heating the sample at 820 °C in nitrogen flow (1 l/min).

4.2.2 Ordered mesoporous silica

Reagents were inserted into an autoclave and synthesis was carried out at 100 °C (SBA-15 and MCM-41) and 110 °C (Al-SBA-15). After the completion of the synthesis, the material was washed, dried and calcined at 500 °C–600 °C. All the mesoporous silica samples were provided by the Department of Chemical Engineering, Åbo Akademi, Turku, Finland.

4.2.3 Loading

PSi particles were loaded with ibuprofen with the immersion method (IV). The particles were immersed in an ethanol solution of ibuprofen (350 mg/ml). After one hour of immersion, the particles were filtered out of the solution and dried at 65°C. GhA was loaded with a similar method. The peptide was dissolved in methanol and sonication was used to ensure homogeneous loading. The drying was performed at room temperature.

4.2.4 Analyses

Thermogravimetry was utilized to measure the drug loading degree in IV and V. Samples were heated up to 700 °C or 800 °C at 20 °C/min in a nitrogen flow of 200 ml/min.

DSC was used to measure melting of ibuprofen in PSi (IV) and melting/freezing behavior of water in MCM-41 and SBA-15 (III). Melting of ibuprofen was measured by heating the sample from -60 °C to 115 °C with heating rate 10 °C/min. To measure freezing/melting of water in mesoporous silica, the porous powders were mixed with water with mass ratios of 1:3 or 1:2 (porous silica: water) and the samples were sealed in aluminum crucibles. Freezing of water was measured by cooling the sample from -0.5 °C to -70 °C and melting of water from -70 °C to 10 °C at a cooling/heating rate of 1 °C/min. The water outside the pores was frozen prior to the measurement. All DSC measurements were conducted under nitrogen flow (40 ml/min).

In all of the articles, mesoporous samples were characterized by gas sorption. Adsorption and desorption of nitrogen were

performed at liquid nitrogen temperature. The pore size was calculated from desorption branch using BJH-theory and surface area from adsorption branch using BET theory. Total pore volume was calculated from a single adsorption point after capillary condensation in mesopores. The primary mesopore volume was calculated with the BJH theory and micropore volume by t-plot analysis (III).

The thickness of the oxide layer was estimated by measuring the pore size of the of oxidized PSi samples by gas sorption before and after dissolving the oxide by HF (II).

X-ray diffraction measurements were preformed with Bragg-Brentano geometry. In articles I and III, powdered samples were compressed on a sample holder, whereas in article II, PSi films were used in a horizontal position (reflection configuration) or vertical position (transmission configuration).

The pore morphology was imaged with SEM. Samples were measured as such, without metal coating. The cross-section of PSi films was imaged from freshly fractured surface (II) whereas mesoporous silica samples were imaged in a powder form (III).

FTIR was used to characterize the surface of PSi in article II. The FTIR spectra were measured in the transmission mode through PSi films. The spectra were recorded in a range from 500 cm^{-1} to 4000 cm^{-1} with resolution 4 cm^{-1}.

Isothermal titration microcalorimetry was used to measure adsorption enthalpy of model drug cinnarizine on oxidized PSi surfaces in the article II. Prior to the measurements, ethanol was added into sample and reference ampoules and PSi microparticles into sample ampoule. The measurements were conducted by injecting the ethanol solution of cinnarizine simultaneously into sample and reference ampoules and measuring the difference in the heat flow signals between the ampoules. Because the only difference between the sample and reference sides was the presence of PSi in the sample ampoule, the recorded heat flow signal was interpreted to arise from energetic interactions between PSi and cinnarizine.

5 Results and discussion

5.1 ENLARGEMENT OF PORES IN POROUS SILICON BY ANNEALING (I)

Therapeutic molecules that can be loaded into PSi vary in size. The size of small molecules can be less than a nanometer whereas proteins can be tens of nanometers in size. Therefore, in order to utilize PSi as a carrier for a wide variety of molecules, also the size of the pores has to be adjustable. Pores of different sizes can be produced by electrochemical etching. However, etching pores in a wide range of pore sizes often encounters practical difficulties. Such difficulties can involve purchasing Si wafers with different doping levels, using high current densities in etching or using different etching setup (e.g. etching with backside illumination). Because of these difficulties, it is practical to perform etching with a standard method and to adjust the pore size after etching. Annealing hydrogen terminated PSi in an inert atmosphere is a useful method for such adjustment.

The effect of annealing on PSi was studied to utilize annealing for controlled enlargement of pores. It was found that the pore size could be controlled from 10 nm up to 80 nm by adjusting the annealing temperature between 400 °C and 900 °C (Fig. 5). The higher the temperature, the larger was the pore size. The enlargement of the pores was found to be sensitive towards the porosity of PSi. The pore size of highly porous (83 %) PSi experienced significantly larger changes compared with PSi with lower porosity (70 %) (Fig. 5).

The lower limit of annealing temperature at which structural changes are observed coincides with those reported in the literature [28]. The extent of pore enlargement was higher than observed by Müller et al. which is easily explained by the low porosity (20 %) of their material [27]. However, the calculated

activation energies were similar to the ones obtained by Müller et al. despite the different porosities.

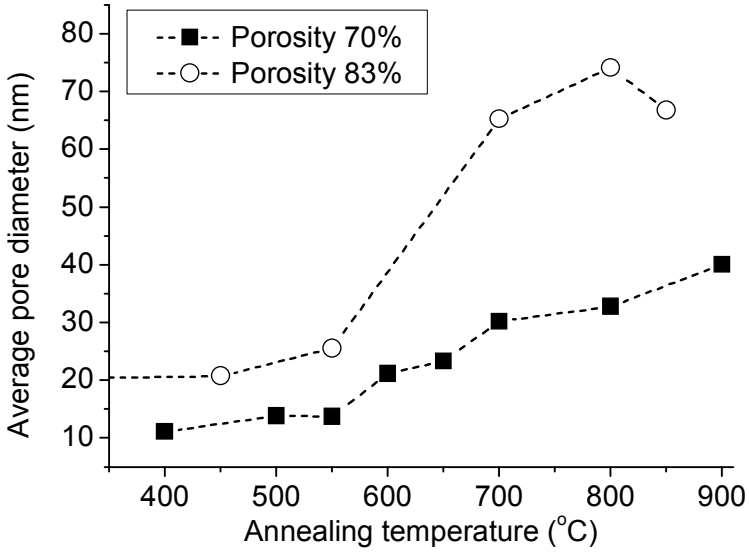

Figure 5. *The effect of annealing temperature on the pore size of porous silicon. The results of two samples with different initial porosities (70 % and 83 %) are presented.*

In addition to the increase in the pore size, also the width of the pore size distribution increased with the increasing annealing temperature. For example, the full width at half maximum values for Gaussian peaks fitted according to the pore size distributions increased from 8 nm to 48 nm for the sample with a porosity of 70 % annealed at 900 °C. The increase in the width of the pore size distribution is expected because of the randomness of the process of fusing the pores.

The structural changes were completed within 45 min in almost all experiments with no further changes observed with prolonged treatment. The rate of structural changes became faster at high temperatures. The structural changes were completed in 20 min at 800 °C whereas at 400 °C it took 90 min despite the small extent of the changes. Müller et al. reported the changes in the pore diameter to follow simple power law $D \propto t^{\frac{1}{4}}$, where t is time [27]. They observed significant changes in the pore diameter between 60 and 120 min even at annealing

temperatures of 1000 °C and did not observe completion of changes. The significantly slower rate of pore diameter change is most likely due to the low porosity and thicker pore walls in the material used by Müller et al. In order for the coalescence of pores with thick walls to take place, the extent of atomic surface diffusion needs to be much higher compared with the material with thin pore walls.

Surface area was found to decrease as a natural consequence of the enlargement of the pore size. In addition, pore volume decreased with increasing annealing temperature. This is most likely due to closing of the pores, creating pores that are not connected to the external surface.

Changes in crystal structure of PSi caused by annealing were observed by XRD. Large changes in the crystal structure took place at a high annealing temperature. The diffraction intensity from {111} planes was at a minimum at an annealing temperature of 600 °C and was recovered at higher temperatures. Interestingly, diffraction intensity from crystallographic {400} planes was decreased as a function of annealing temperature, almost disappearing at 900 °C. There was no significant change in the baseline level, indicating that no amorphous phase had been formed. Similar results were obtained by Ogata et al. although comparison of results is difficult because of the small number of annealing temperatures used by Ogata et al. [28].

Annealing was found to be a useful method of producing PSi with distinct pore sizes. The resulting pore size can be controlled with annealing temperature. The method is especially beneficial when producing a series of PSi samples with various pore sizes. These results were utilized in article IV to produce a series of PSi samples with distinct pore sizes between 10 nm and 75 nm.

5.2 OXIDATION OF POROUS SILICON (II)

High surface area and pore volume as well as inertness towards guest molecules are beneficial properties for a mesoporous drug carrier. To ensure the inertness, the surface needs to be stabilized which is most often achieved by oxidation. However, oxidation reduces the surface area and the pore volume because of the volume expansion of the surface which occurs during oxidation. Therefore, it was considered desirable to develop an oxidation method that would produce inert surfaces but cause minimal changes on the pore structure.

A large number of oxidation treatments were used to oxidize PSi. The primary aim was to produce surfaces free from hydride groups (Si-H_x) because of their reactivity. The oxidation in the liquid phase without high temperature treatments was found to be unable to produce surfaces completely free from hydrides. This is most likely due to steric hindrances. The surface of PSi has high hydride coverage after production with mono-, di- and trihydrides present at the surface. Oxidation of all hydrides to hydroxyl groups (Si-OH_x) cannot take place because of increasing steric constraints as the oxygen atom is added into the structure. On solid surfaces, Si-OH_3 groups are rarely found and therefore, some hydrides are always left on the surface.

There are reports claiming complete or almost complete removal of hydrides with liquid phase oxidation [129, 130]. It is likely that this discrepancy is due to the thickness of the PSi films used in the FTIR measurements. The films with thickness of ~ 100 μm were used in this work to achieve high sensitivity towards low quantities of chemical species. Thinner films were used in the studies by Fukuda et al. and Li et al. and this might explain why no hydrides were detected.

In order to produce surfaces free of hydrides, it was found necessary to apply a heat treatment. Heat treatment evokes desorption of hydride groups and reordering of the surface, consequently, reducing steric crowding. When there are fewer hydride groups on the surface, it is possible to oxidize the remaining hydride groups.

Three methods involving heat treatments were able to produce hydride-free surfaces: thermal oxidation at 700 °C (sample 1, S1), the combination of thermal oxidation (300 °C) and annealing (1000 °C) (S2), and the combination of thermal oxidation (300 °C), annealing (750 °C) and liquid phase oxidation (S3). These methods were optimized to produce as small changes as possible into the pore structure. A thermally oxidized (300 °C, 120 min) sample TO120 containing hydride groups was produced as a reference.

Structural and chemical properties of samples 1, 2 and 3 were compared (Fig. 6). Sample 1 had a thick oxide surface and the pore volume decreased by a third. Sample 3 exhibited smaller changes in the pore volume and an insignificant change in the pore size. Sample 2 displayed the smallest decrease in the pore volume and an increase in pore diameter. However, further investigation showed that the coverage of the oxide surface was not sufficient to stabilize the surface and the material since the sample experienced chemical changes upon storage under ambient conditions.

The oxide thicknesses are very high compared to the reported growth rate of thermal oxide layer on porous silicon 0.025 nm/min at 800 °C [131]. These values are for oxidation times > 1 h and PSi with wall thickness of 30 nm. The initial rate of oxidation is much higher because of the easier diffusion of oxygen in the structure. Jarvis et al. reported changes in the surface area, pore volume and pore diameter caused by thermal oxidation at various temperatures for 1 h [41]. They showed a decrease in surface area, pore volume and pore diameter with increasing oxidation time, in agreement with the results presented here.

The chemical reactivity of these surfaces towards cinnarizine was evaluated by isothermal titration microcalorimetry. Samples 1 and 3 were found to exhibit small heat of adsorption < 11 kJ/mol (measured heat associated with adsorption per moles of injected cinnarizine) consistent with physisorption of cinnarizine onto the surfaces. Despite the apparent similarity of the surfaces on sample 1 and 2, sample S2 showed high heats of

adsorption (52 kJ/mol) which was interpreted as a sign of a chemical reaction associated with adsorption. The nature of the chemical reaction between cinnarizine and S2 was not determined. The heats of adsorption presented here are a lower limit for the initial heat of adsorption of cinnarizine. The actual values could be higher because all of the cinnarizine from the solution might not adsorb onto the PSi surfaces. In addition, the heats of adsorption were decreasing for subsequent injections, which indicates that if smaller injections were used, the heat of adsorption for the first injection would most likely be higher. The results pointed to low reactivities for S1 and S3, but no general conclusions could be drawn.

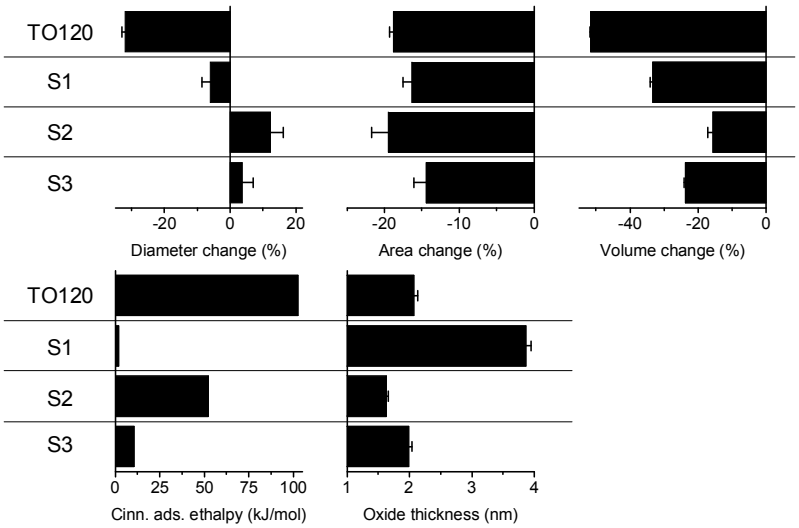

Figure 6. *Changes in properties of PSi caused by oxidation treatments. The changes in pore diameter, surface area and pore volume caused by oxidation treatments are presented. In addition, the adsorption enthalpy of cinnarizine on oxidized PSi surfaces and the thickness of the oxide layer are shown. The samples were oxidized by following treatments TO120: thermal oxidation (300 °C, 120 min), S1: thermal oxidation (700 °C, 7.5 min), S2 thermal oxidation (300 °C, 4 min) + annealing (1000 °C, 20 min) and S3: thermal oxidation (300 °C, 4 min) + annealing (750 °C, 30 min) + liquid phase oxidation (with last two steps repeated).*

The comparison between samples thermally oxidized at 700 °C for 7.5 min (S1) and at 300 °C for 120 min (TO120) was

particularly interesting. Although S1 had a thicker oxide surface, it exhibited a smaller decrease in pore volume and diameter. This could be explained by a swelling of the silicon skeleton during the oxidation at 700 °C facilitated by the higher ductility of the silicon. Whereas at 300 °C, the oxide had to grow towards the pore centers, at 700 °C the swelling could partially accommodate the volume expansion. This hypothesis was supported by XRD measurements showing higher increase in the size of voids in the silicon crystal in S1 sample compared with TO120 sample.

A high temperature thermal oxidation (S1) was found to be a beneficial method of oxidizing PSi. It produced inert surfaces and thick oxide layers. The growth of a thick oxide layer could be partially accommodated by swelling of the structure, and therefore there were no dramatic changes in the pore structure. The combination of thermal oxidation, annealing and liquid phase oxidation (S3) preserved the pore structure better than a high temperature oxidation. However, before applying this method one should carefully consider whether the benefits in the structure outweigh the longer time required for sample preparation.

5.3 CHARACTERIZING U-SHAPED PORES IN SBA-15 (III)

The pore structure of mesoporous materials is important in drug delivery applications because it affects loading and release of drugs. SBA-15 has a tendency to form u-shaped pores to varying degrees. U-shaped pores (Fig. 7) do not simply extend through the particle but are folded back into the particle at the surface, forming a u-shape. This increases the length of the pore compared to straight pores that go directly through the particle with openings at both ends. The increase in the particle size has been found to decrease the release rate of a drug which is most likely related to the increase in the pore length. Therefore, one can hypothesize that the u-shaped pores would have a similar release hindering effect. However, it is difficult to quantify the

amount of these pores. Although they can be observed with SEM it is very difficult to obtain any quantifiable estimate of the proportions of straight and u-shaped pores.

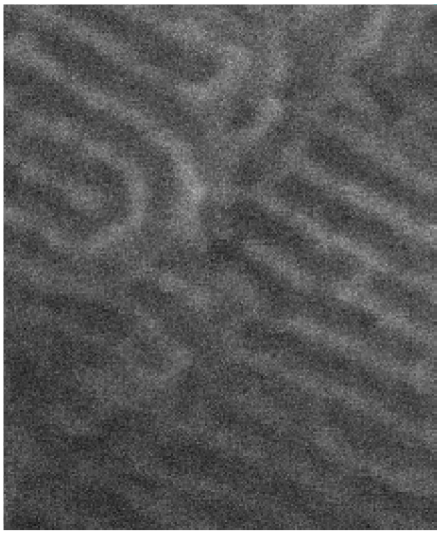

Figure 7. *SEM image showing u-shaped pores in SBA-15.*

In article III, a novel method of quantifying the u-shaped pores was developed. This method is based on measuring freezing and melting of water in the pores by DSC. SBA-15 was found to exhibit an unusual freezing–melting hysteresis where freezing produced a single peak but the melting process was split into two separate peaks, centered at different temperatures (Fig. 8). There is a previous mention of this kind of hysteresis in the literature but its origins were not explained [132]. We assigned these two melting peaks to the melting of water in the u-shaped pores and straight pores according to the following explanation (Fig. 8). When the temperature of the SBA-15 with pores filled with ice is increased, the ice in the curved part of the u-shaped pore will melt at the lowest temperatures. This can be either due to the high curvature of the outermost curved wall of the pore (innermost wall forms a saddle surface with a low local curvature) or defects in the ice crystal caused by the curve of the pore. As soon as the curved part has melted, a new hemispherical solid-liquid interface is formed. This interface has

a high curvature as compared with the cylindrical surface of the ice in the straight parts of the pore. This high curvature makes the interface unstable at the prevailing temperature and the ice in the straight parts of the u-shaped pores melts instantaneously after the melting of the ice in the curved part. In the straight pores, melting is initiated at a higher temperature, i.e. when the cylindrical interface of the ice becomes unstable. Therefore, the peak at a lower temperature represents melting of ice in all pores containing u-shapes and the peak at higher temperatures represents melting in the straight pores. The ratio of volume in the two types of pores is obtained by calculating the ratio of the peak areas, since the area of a melting peak is equal to the melting enthalpy.

Two melting peaks would also be observed if there were two distinct pore sizes but this would produce two freezing peaks as well, which was not observed. Instead, only one freezing peak was detected, i.e. freezing takes place at the same temperature in both pore types, consistent with the above interpretation. The freezing is initiated by nucleation at bulk ice at the pore openings and the pore openings are of the same size in both straight pores and u-shaped pores. The shape of the solid–liquid interface is hemispherical and, therefore, the freezing temperature is lower compared with the melting temperature of ice in straight pores which is determined by of the curvature of the cylindrical interface.

Interestingly, similar behavior was not observed in nitrogen sorption measurements, although analysis of freezing and desorption as well as melting and adsorption usually provide similar results. A significant difference between the two methods is that in melting/freezing experiments there is an ordered phase (ice) present whereas in the gas sorption none of the phases are ordered. This could mean that defects in the ice crystals are responsible for the initiation of melting in the u-shaped pores.

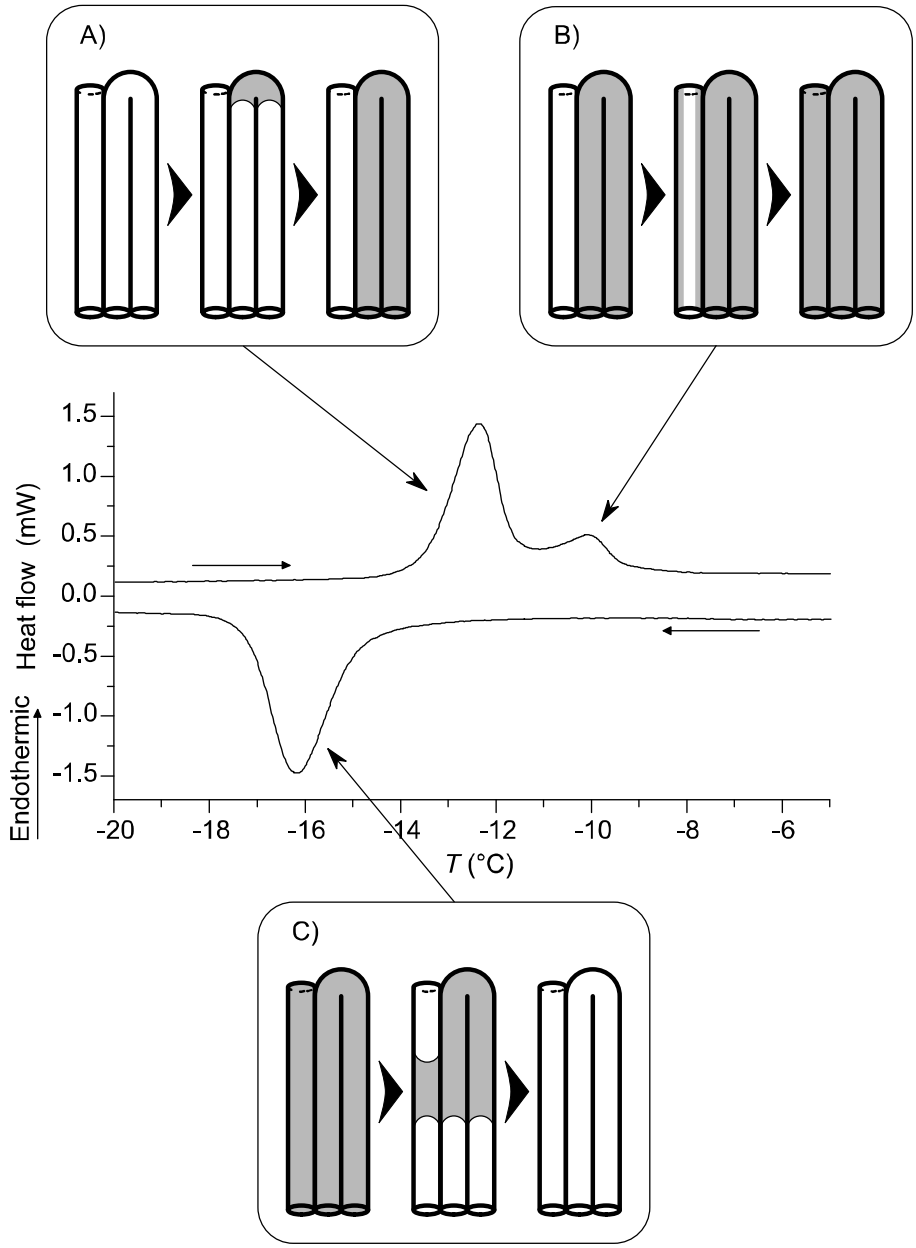

Figure 8. *Melting and freezing of water in the pores of SBA-15 measured by DSC. The schematic reveals the mechanism behind the hysteresis phenomenon: A) melting of ice in u-shaped pores, B) melting of ice in the straight pores and C) freezing in both types of pores.*

Different proportions of u-shaped and straight pores were observed in different SBA-15 materials. The fraction of pore volume in u-shaped pores was (65 ± 1) % and (27 ± 2) % in siliceous SBA-15 and Al-SBA-15, respectively. A similar phenomenon was not observed with MCM-41.

Since no other method can be used to measure proportions of these pores, the values obtained here could not be quantitatively validated. A qualitative support was obtained with SEM imaging which revealed that more u-shaped pores could be observed in SBA-15 than in Al-SBA-15. However, further support for the validity of the method is not available.

5.4 PHYSICAL STATE OF DRUGS IN POROUS SILICON (IV)

The majority of articles about drug delivery with mesoporous materials describe systems in which the drug is present in an amorphous form. The amorphicity of the drug is often due to the small size of the pores preventing crystallization. If there are sufficiently large pores, then drugs are able to crystallize. However, crystalline forms of drugs in the pores are not well studied. It is important to be aware of the physical state of drugs in the pores because it may affect physical and chemical stability of the drugs and their release from the pores.

Eight PSi batches were produced with different pore sizes by annealing at different temperatures and by surface oxidation followed by etching the oxide with HF. The pore diameters were in the range from 10 nm to 75 nm. Each of the eight batches was divided into three samples with different surfaces: thermally oxidized (TO), thermally carbonized (TC) and as-anodized (AA) which is the hydrogen terminated surface. These samples were loaded with ibuprofen and the melting of ibuprofen was measured with DSC.

Ibuprofen was found to be present in crystalline state in all the samples. Outside the pores, crystalline ibuprofen was only observed in two samples and at minor amounts (< 0.1 % of total amount of ibuprofen in the sample). Inside the pores, crystalline

ibuprofen was found in all of the samples. However, in the smallest pores, crystallization was found to be a slow process that could take several weeks to reach a stable state. After reaching the stable state, no further change was detected even after several months.

A clear trend was observed, when the measured melting enthalpy of ibuprofen was divided by the mass of ibuprofen in the sample. The smaller the pores, the lower was the specific melting enthalpy and the lower was the crystallinity of ibuprofen. The crystallinity of ibuprofen varied between 39 % and 94 %. This was assumed to be because of the non-crystalline δ-layer between the pore wall and the drug crystal. In order to test this hypothesis and to evaluate the thickness of the layer, a simple geometrical model of the system was devised (Fig. 9). The pores were assumed to be cylindrical with diameter D and the drug was assumed to fill the pore where it existed i.e. no parts of the pores contained only a layer of the drug on the pore walls. Ibuprofen at the center of the pores was in the crystalline state and there was a δ-layer with constant thickness (δ) between the crystalline core and the pore wall. With this geometrical model, and also assuming the specific melting enthalpy of the crystalline part Δh to be equal to the bulk value (125.9 J/g), the following equation between the measured melting enthalpy (ΔH) and δ was derived:

$$\frac{\Delta H}{m} = \Delta h \left(1 - \frac{2\delta}{D}\right)^2, \qquad (4.1)$$

where m is the mass of ibuprofen in the sample. The values for δ were obtained by plotting the $\Delta H/m$ versus D and fitting the equation (4.1) to the data points separately for each surface type (Fig. 10). The thickness of the δ-layer was found to be 1.2 nm, 1.5 nm and 2.0 nm on AA, TO and TC surfaces, respectively. The values of δ can be considered as an indication of the strength of the drug–pore wall interactions. The stronger are the interactions, the further from the surface the effect extends and the thicker is the δ-layer.

This work is the first report of the δ-layer thicknesses for drugs in mesoporous materials. Azais et al. reported that, in addition to the crystalline phase, some disordered ibuprofen

was always detected in the 11.6 nm wide pores of MCM-41 [133]. The thickness of δ-layer has been previously reported for simple molecules which are usually used as probe molecules in thermoporometry [65]. The reported thicknesses are typically in the range of 2 – 4 monolayers. The present results suggest a δ-layer of 1 – 4 monolayers (size of an ibuprofen molecule is approximately 1.2 nm x 0.8 nm x 0.5 nm [133]).

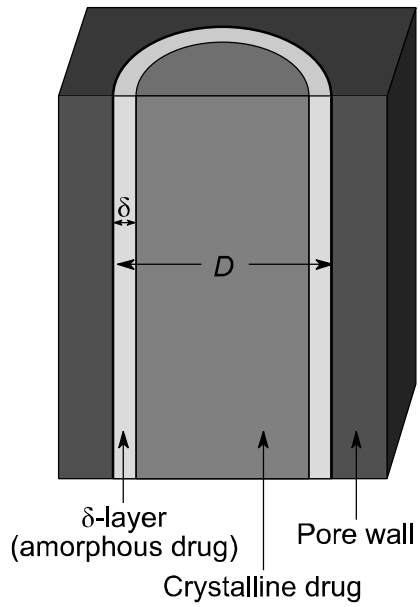

Figure 9. *The geometrical model of ibuprofen in pores of PSi devised in order to derive the equation (4.1).*

The nature of interactions between ibuprofen and the PSi surfaces was not determined, but some clues could be obtained by zeta potential measurements. The thickest δ-layer was found with the TC surface, which is expected to be oxidized silicon carbide surface. This surface had the greatest negative zeta potential of the three tested surfaces. The TO surface is partially oxidized and had the second most negative zeta potential. The HT surface on the other hand, was only slightly oxidized by the short exposure with air and had the least negative zeta potential as well as the thinnest δ-layer. Therefore, it is possible that the

carboxylic group of ibuprofen is forming hydrogen bonds with the surface oxides of PSi.

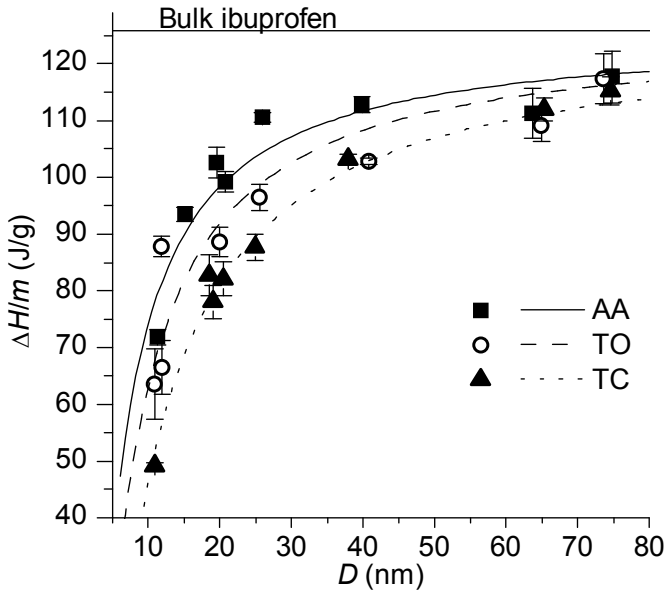

Figure 10. *Graph showing the specific melting enthalpy of ibuprofen in the pores of PSi versus the pore diameter. Equation 4.1 is fitted to the data points to obtain the thickness of the δ-layer.*

The validity of the assumption for Δh was tested by using it as a fitting parameter. The values obtained were between 121 J/g and 128 J/g and in good agreement with the assumption. The values of δ from this fitting were not significantly different from those obtained with fixed Δh.

The geometrical model is not totally valid especially for non-annealed samples. It is well known that the pores in PSi are not cylindrical, as assumed in the model, but have rather irregular, branched pore walls which are likely to be smoothed by annealing. However, the fittings were reasonably good, which seems to indicate that the errors due to the model were moderate.

It was shown that both pore size and surface chemistry of the carrier affect the crystallinity of ibuprofen in the pores. Crystallinity is known to affects the dissolution rate of

macroscopic drug particles and, therefore, it seems reasonable to expect that crystallinity would also influence the release of drugs from mesoporous carriers. Indeed, it has been recently observed that drug in a crystalline form in the pores was released slower than a drug in an amorphous form [101]. However, our unpublished work has shown very fast release rates of drugs in crystalline form from large pores.

There are several parameters affecting the release behavior of drugs from a mesoporous carrier. The pore size affects crystallinity and also diffusion of drugs from the pores. Furthermore, the surface chemistry of the carrier not only influences the crystallinity but also the release of drug molecules that are in contact with the surface. Therefore, more work will need to be done to truly uncover the optimal properties of the mesoporous drug carriers.

5.5 POROUS SILICON IN SUSTAINED DELIVERY OF PEPTIDES

Peptides are promising therapeutic agents for several severe illnesses. However, their applicability is often limited by their short duration of activity *in vivo*. Therefore, there is a need for novel delivery methods providing sustained delivery of peptides in an active form.

Delivery of a peptide GhA from THCPSi microparticles was studied *in vivo*. THCPSi particles were chosen because of the stability of the surface preventing chemical reactions between the surface and the peptide, and because of their hydrophobic surface. Peptide can be bound on the hydrophobic surface by hydrophobic interaction and therefore a sustained release in an aqueous medium can be achieved. The used particles had large enough pore size (> 11 nm) to easily accommodate the peptide molecules with molecular weight < 1000 g/mol and high enough surface area and pore volume to provide loading degree > 15 %.

Animal models offer the most realistic way to study the applicability of the peptide loaded carriers. Furthermore, by studying the physiological responses to the released peptide, it

is possible to show in addition to the release of the peptide, that the peptide remains biologically active.

Physiological responses to the peptide were followed by observing the food intake in mice and measuring the blood pressure in rats after injections of GhA loaded THCPSi microparticles. A vehicle, GhA solution or unloaded THCPSi particles were injected as controls. The injections were given subcutaneous (under skin), which is a suitable route because it enables the adsorption of peptides (contrary to oral route with most peptides), enables usage of > 38 μm particles and can be done easily to conscious animals.

The effect of GhA solution on food intake lasted for 4 h. However, GhA-loaded THCPSi particles were found to inhibit food intake at the beginning of the experiment and between 7 h and 17 h (Fig. 11). Cumulative food intake between 7 h and 17 h was 0.203 g/g and 0.229 g/g (grams of food per grams of body weight) for GhA-loaded THCPSi and GhA solution, respectively. The loaded GhA maintained relatively stable elevation in blood pressure in rats for 9h whereas the effect of GhA solution was very high at 1 h but decreased back to the baseline in 10 h (Fig. 11).

Plasma cytokine levels were also tested after administration of unloaded THCPSi particles. Elevated levels of cytokines are indicative of inflammation or infections in the organism. Significantly ($p < 0.05$) elevated cytokine levels were found only for one cytokine at one time point. However, since a total of 30 time points was tested; this is likely to be an experimental artifact.

These results indicated that THCPSi particles were releasing an active form of GhA in a sustained manner without evoking an inflammatory response. The physiological response to the GhA-loaded THCPSi was rather weak and the duration of the effect was not as long as would be required for the formulation to be commercially interesting. Other techniques have been reported to provide more sustained release of peptides after subcutaneous injections [134, 135]. However, this was the first

report of *in vivo* peptide delivery with PSi, opening a pathway to further development in this field.

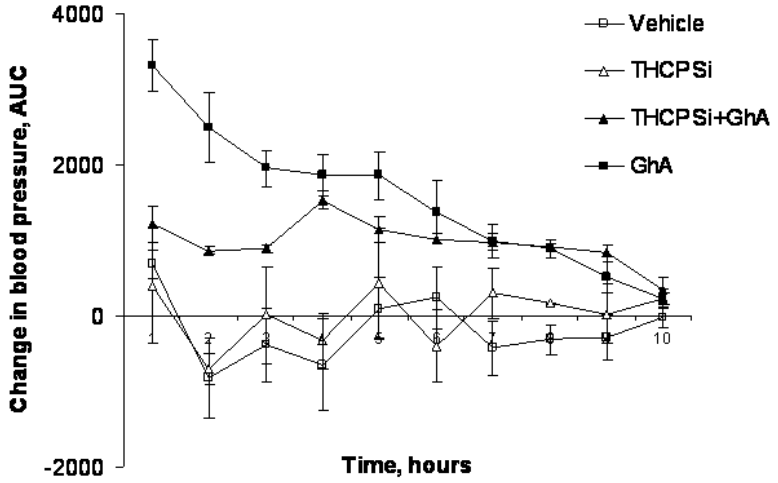

Figure 11. *Results of peptide delivery experiments showing change in blood pressure in rats after subcutaneous administration of GhA, GhA loaded THCPSi microparticles (THCPSi+GhA), vehicle and unloaded THCPSi microparticles (THCPSi).*

6 Conclusions

Several aspects of development of mesoporous materials as drug delivery agents were studied, from material production to characterization and finally to *in vivo* delivery experiments.

Thermal annealing of PSi in an inert atmosphere was found to be a suitable method of increasing pore size from 10 nm up to 80 nm in a controlled manner. The pore size could be manipulated by adjusting the annealing temperature. The initial porosity of the sample was found to have a major impact on the extent of the pore size increase.

A wide variety of oxidation methods was evaluated for a stabilization of PSi. Liquid phase oxidation was not able to produce hydride-free surfaces. Oxidation at high temperatures for a relatively short time was found to be a beneficial method because it caused relatively minor changes in the pore structure and generated surfaces that were not found to react with the model drug. Smaller changes in the pore structure were achieved with an elaborate method comprising of thermal oxidation, annealing and liquid phase oxidation.

A novel method of quantifying u-shaped pores in SBA-15 was developed. The method was based on the unique hysteresis phenomenon occurring between melting and freezing of water inside the pores. No other method is known to be capable of quantifying this property of SBA-15.

The physical state of ibuprofen in PSi with various pore sizes and surface chemistries was characterized. The drug was found to crystallize at the center of the pores and a non-crystalline layer was formed between the crystalline part and the pore wall. The thickness of this layer was dependent on the surface chemistry of the pores. A method was developed to measure the thickness of this layer. By varying the pore size and the surface chemistry, the crystallinity of ibuprofen varied between 39 % and 94 %.

Thermally hydrocarbonized PSi microparticles were shown to be able to deliver a biologically active form of a peptide ghrelin antagonist in a sustained manner *in vivo*. The peptide loaded carrier exhibited sustained effect on both food intake in mice and blood pressure in rats after subcutaneous administration. In addition, the PSi microparticles were not found to evoke any inflammatory reactions.

These studies highlight the wide range of elements involved in the development of mesoporous drug delivery systems. From the production of the porous structure and design of the surface chemistry to detailed characterization of such systems and finally to the application of the systems in living organisms. The pore structure and surface chemistry cannot be designed independently as the modifications of surface chemistry can have significant influence on the pore structure. Furthermore, the pore structure and surface chemistry influence the physical and chemical forms of the loaded drug. A thorough characterization of the drug carrier and the drug in the carrier is essential in understanding the delivery system. Conventional analysis techniques are not always sufficient to detect all the essential features of these delivery systems.

The knowledge related to mesoporous drug delivery systems is increasing rapidly as new research papers in this field are being published daily. However, there is still plenty of room for new research. The present work provides some loose ends that motivate future studies. The evolution of the structure of PSi at the atomic level during annealing and thermal oxidation requires more systematic studies in order that it can be understood in detail. Moreover, evaluating the effect of pore size, surface chemistry and thickness of the δ-layer on the release profile of poorly soluble drugs would be particularly interesting and might provide further insights in these drug delivery systems. The effect of u-shaped pores on the release rate of drugs has not been determined so far, although this kind of study would be now feasible on the basis of the present results.

A proof of concept for sustained delivery peptides with PSi was provided in this work. Further development is needed in order to fully realize the potential of the delivery system. Indeed, the work has since then been continued by studying the formulations of peptides and PSi and by providing delivery systems capable of sustaining the release of peptides for up to four days [127, 136].

Despite the vast interest in mesoporous drug delivery systems, commercial products have not reached the markets so far. It seems very likely that such products will emerge as the current academic knowledge is now being utilized in commercial developments by several companies such as Formac Pharmaceuticals and pSivida.

7 References

[1] M. S. Ku and W. Dulin, "A biopharmaceutical classification-based Right-First-Time formulation approach to reduce human pharmacokinetic variability and project cycle time from First-In-Human to clinical Proof-Of-Concept," *Pharm. Dev. Technol.* **17,** 285-302 (2012).

[2] Y. Kawabata, K. Wada, M. Nakatani, S. Yamada and S. Onoue, "Formulation design for poorly water-soluble drugs based on biopharmaceutics classification system: Basic approaches and practical applications," *Int. J. Pharm.* **420,** 1-10 (2011).

[3] N. Blagden, M. de Matas, P. T. Gavan and P. York, "Crystal engineering of active pharmaceutical ingredients to improve solubility and dissolution rates," *Adv. Drug Deliv. Rev.* **59,** 617-630 (2007).

[4] T. Loftsson, P. Jarho, M. Másson and T. Järvinen, "Cyclodextrins in drug delivery," *Expert Opin. Drug Deliv.* **2,** 335-351 (2005).

[5] S. Janssens and G. Van Den Mooter, "Review: Physical chemistry of solid dispersions," *J. Pharm. Pharmacol.* **61,** 1571-1586 (2009).

[6] V. A. Saharan, V. Kukkar, M. Kataria, M. Gera and P. K. Choudhury, "Dissolution enhancement of drugs part II: Effect of carriers," *Int. J. Health Res.* **2,** 207-223 (2009).

[7] L. R. Brown, "Commercial challenges of protein drug delivery," *Expert Opin. Drug Deliv.* **2,** 29-42 (2005).

[8] M. Werle and A. Bernkop-Schnürch, "Strategies to improve plasma half life time of peptide and protein drugs," *Amino Acids* **30,** 351-367 (2006).

[9] P. Jani, P. Manseta and S. Patel, "Pharmaceutical approaches related to systemic delivery of protein and peptide drugs: An overview," *Int. J. Pharm. Sci. Rev. Res.* **12,** 42-52 (2012).

[10] J. Salonen, A. Kaukonen, J. Hirvonen and V. P. Lehto, "Mesoporous silicon in drug delivery applications," *J. Pharm. Sci.* **97,** 632-653 (2008).

[11] M. Van Speybroeck, V. Barillaro, T. D. Thi, R. Mellaerts, J. Martens, J. Van Humbeeck, J. Vermant, P. Annaert, G. Van Den Mooter and P. Augustijns, "Ordered mesoporous silica material SBA-15: A broad-spectrum formulation platform for poorly soluble drugs," *J. Pharm. Sci.* **98,** 2648-2658 (2009).

[12] K. Sing, D. Everett, R. Haul, L. Moscou, R. PierottiI, J. Rouquerol and T. Siemieniewska, "Reporting Physisorption Data for Gas Solid Systems with Special Reference to the Determination of Surface-Area and Porosity (Recommendations 1984)," *Pure Appl. Chem.* **57,** 603-619 (1985).

[13] P. Van Der Voort, C. Vercaemst, D. Schaubroeck and F. Verpoort, "Ordered mesoporous materials at the beginning of the third millennium: New strategies to create hybrid and non-siliceous variants," *Phys. Chem. Chem. Phys.* **10,** 347-360 (2008).

[14] A. Uhlir, "Electrolytic Shaping of Germanium and Silicon," *Bell System Tech. J.* **35,** 333-347 (1956).

[15] A. Uhlir and I. Uhlir, "Historical perspective on the discovery of porous silicon," *Phys. Status Solidi C* **2,** 3185-3187 (2005).

[16] Y. Watanabe and T. Sakai, "Application of a thick anode film to semiconductor devices," *Rev. Elec. Commun. Lab.* **19,** 899-903 (1971).

[17] L. T. Canham, "Silicon quantum wire array fabrication by electrochemical and chemical dissolution of wafers," *Appl. Phys. Lett.* **57,** 1046-1048 (1990).

[18] L. T. Canham, "Bioactive silicon structure fabrication through nanoetching techniques," *Adv. Mater.* **7,** 1033-1037 (1995).

[19] G. Korotcenkov and B. K. Cho, "Silicon porosification: State of the art," *Crit. Rev. Solid State Mater. Sci.* **35,** 153-260 (2010).

[20] K. W. Kolasinski, "Charge transfer and nanostructure formation during electroless etching of silicon," *J. Phys. Chem. C* **114,** 22098-22105 (2010).

[21] A. Loni, D. Barwick, L. Batchelor, J. Tunbridge, Y. Han, Z. Y. Li and L. T. Canham, "Extremely high surface area metallurgical-grade porous silicon powder prepared by metal-assisted etching," *Electrochem. Solid-State Lett.* **14,** K25-K27 (2011).

[22] K. W. Kolasinski, "Etching of silicon in fluoride solutions," *Surf. Sci.* **603,** 1904-1911 (2009).

[23] J. N. Chazalviel, R. B. Wehrspohn and F. Ozanam, "Electrochemical preparation of porous semiconductors: from phenomenology to understanding," *Mat. Sci. Eng. B* **69-70,** 1-10 (2000).

[24] V. Lehmann, R. Stengl and A. Luigart, "On the morphology and the electrochemical formation mechanism of mesoporous silicon," *Mat. Sci. Eng. B* **69,** 11-22 (2000).

[25] V. Lehmann and U. Gösele, "Porous silicon formation: A quantum wire effect," *Appl. Phys. Lett.* **58,** 856-858 (1991).

[26] R. Herino, A. Perio, K. Barla and G. Bomchil, "Microstructure of Porous silicon and its evolution with temperature," *Mater. Lett.* **2,** 519-523 (1984).

[27] G. Müller, M. Nerding, N. Ott, H. P. Strunk and R. Brendel, "Sintering of porous silicon," *Phys. Status Solidi A* **197,** 83-87 (2003).

[28] Y. H. Ogata, N. Yoshimi, R. Yasuda, T. Tsuboi, T. Sakka and A. Otsuki, "Structural change in p-type porous silicon by thermal annealing," *J. Appl. Phys.* **90,** 6487-6492 (2001).

[29] A. Halimaoui, Y. Campidelli, A. Larre and D. Bensahel, "Thermally-Induced Modifications in the Porous Silicon Properties," *Phys. Status Solidi B* **190,** 35-40 (1995).

[30] J. M. Buriak, "Organometallic chemistry on silicon and germanium surfaces," *Chem. Rev.* **102,** 1271-1308 (2002).

[31] J. Salonen, V. P. Lehto and E. Laine, "The room temperature oxidation of porous silicon," *Appl. Surf. Sci.* **120,** 191-198 (1997).

[32] E. C. Wu, J. S. Andrew, A. Buyanin, J. M. Kinsella and M. J. Sailor, "Suitability of porous silicon microparticles for the long-term delivery of redox-active therapeutics," *Chem. Commun.* **47,** 5699-5701 (2011).

[33] M. P. Stewart and J. M. Buriak, "New approaches toward the formation of silicon-carbon bonds on porous silicon," *Comments Inorg. Chem.* **23,** 179-203 (2002).

[34] J. Salonen, V. P. Lehto and E. Laine, "Thermal oxidation of free-standing porous silicon films," *Appl. Phys. Lett.* **70,** 637-639 (1997).

[35] D. B. Mawhinney, J. A. Glass and J. T. Yates, "FTIR study of the oxidation of porous silicon," *J. Phys. Chem. B* **101,** 1202-1206 (1997).

[36] L. Debarge, J. P. Stoquert, A. Slaoui, L. Stalmans and J. Poortmans, "Rapid thermal oxidation of porous silicon for surface passivation," *Mater. Sci. Semicond. Process.* **1,** 281-285 (1998).

[37] J. E. Bateman, R. D. Eagling, B. R. Horrocks, A. Houlton and D. R. Worrall, "Rôle for organic molecules in the

oxidation of porous silicon," *Chem. Commun.* **1997,** 2275-2276 (1997).

[38] U. Frotscher, U. Rossow, M. Ebert, C. Pietryga, W. Richter, M. G. Berger, R. Arens-Fischer and H. Münder, "Investigation of different oxidation processes for porous silicon studied by spectroscopic ellipsometry," *Thin Solid Films* **276,** 36-39 (1996).

[39] R. Czaputa, R. Fritzl and A. Popitsch, "Anomalous luminescence degradation behaviour of chemically oxidized porous silicon," *Thin Solid Films* **255,** 212-215 (1995).

[40] M. Schoisswohl, H. J. von Bardeleben, V. Morazzani, A. Grosman, C. Ortega, S. Frohnhoff, M. G. Berger and H. Münder, "Analysis of the surfaces structure in porous Si," *Thin Solid Films* **255,** 123-127 (1995).

[41] K. L. Jarvis, T. J. Barnes, A. Badalyan, P. Pendleton and C. A. Prestidge, "Impact of thermal oxidation on the adsorptive properties and structure of porous silicon particles," *J. Phys. Chem. C* **112,** 9717-9722 (2008).

[42] J. Salonen, E. Laine and L. Niinistö, "Thermal carbonization of porous silicon surface by acetylene," *J. Appl. Phys.* **91,** 456-461 (2002).

[43] J. Salonen, M. Björkqvist, E. Laine and L. Niinistö, "Stabilization of porous silicon surface by thermal decomposition of acetylene," *Appl. Surf. Sci.* **225,** 389-394 (2004).

[44] V. Chiola, J. Ritsko and C. Vanderpool, "Process for producing low-bulk density silica," U.S. patent 3,556,725 (1971).

[45] F. Di Renzo, H. Cambon and R. Dutartre, "A 28-year-old synthesis of micelle-templated mesoporous silica," *Micropor. Mesopor. Mat.* **10,** 283-286 (1997).

[46] T. Yanagisawa, T. Shimizu, K. Kuroda and C. Kato, "The preparation of alkyltrimethylammonium-kanemite

complexes and their conversion to microporous materials," *Bull. Chem. Soc. Jpn.* **63,** 988-992 (1990).

[47] C. T. Kresge, M. E. Leonowicz, W. J. Roth, J. C. Vartuli and J. S. Beck, "Ordered Mesoporous Molecular-Sieves Synthesized by a Liquid-Crystal Template Mechanism," *Nature* **359,** 710-712 (1992).

[48] D. Y. Zhao, J. L. Feng, Q. S. Huo, N. Melosh, G. H. Fredrickson, B. F. Chmelka and G. D. Stucky, "Triblock copolymer syntheses of mesoporous silica with periodic 50 to 300 angstrom pores," *Science* **279,** 548-552 (1998).

[49] M. J. Rosen, *Surfactants and Interfacial Phenomena* (Wiley, Hoboken, 2004).

[50] K. Flodström, H. Wennerström and V. Alfredsson, "Mechanism of mesoporous silica formation, a time-resolved NMR and TEM study of silica-block copolymer aggregation," *Langmuir* **20,** 680-688 (2004).

[51] K. Flodström, C. V. Teixeira, H. Amenitsch, V. Alfredsson and M. Lindén, "In situ synchrotron small-angle X-ray scattering/X-ray diffraction study of the formation of SBA-15 mesoporous silica," *Langmuir* **20,** 4885-4891 (2004).

[52] S. Ruthstein, J. Schmidt, E. Kesselman, Y. Talmon and D. Goldfarb, "Resolving intermediate solution structures during the formation of mesoporous SBA-15," *J. Am. Chem. Soc.* **128,** 3366-3374 (2006).

[53] D. Y. Zhao, Q. S. Huo, J. L. Feng, B. F. Chmelka and G. D. Stucky, "Nonionic triblock and star diblock copolymer and oligomeric surfactant syntheses of highly ordered, hydrothermally stable, mesoporous silica structures," *J. Am. Chem. Soc.* **120,** 6024-6036 (1998).

[54] Y. Wan and D. Zhao, "On the controllable soft-templating approach to mesoporous silicates," *Chem. Rev.* **107,** 2821-2860 (2007).

[55] A. Taguchi and F. Schüth, "Ordered mesoporous materials in catalysis," *Micropor. Mesopor. Mat.* **77,** 1-45 (2005).

[56] M. Imperor-Clerc, P. Davidson and A. Davidson, "Existence of a microporous corona around the mesopores of silica-based SBA-15 materials templated by triblock copolymers," *J. Am. Chem. Soc.* **122,** 11925-11933 (2000).

[57] S. N. Che, K. Lund, T. Tatsumi, S. Iijima, S. H. Joo, R. Ryoo and O. Terasaki, "Direct observation of 3D mesoporous structure by scanning electron microscopy (SEM): SBA-15 silica and CMK-5 carbon," *Angew. Chem. Int. Ed. Engl.* **42,** 2182-2185 (2003).

[58] Y. Yue, A. Gédéon, J. L. Bonardet, N. Melosh, J. B. D'Espinose and J. Fraissard, "Direct synthesis of AlSBA mesoporous molecular sieves: Characterization and catalytic activities," *Chem. Commun.* **1999,** 1967-1968 (1999).

[59] A. Endo, M. Yamada, S. Kataoka, T. Sano, Y. Inagi and A. Miyaki, "Direct observation of surface structure of mesoporous silica with low acceleration voltage FE-SEM," *Colloids Surf. A* **357,** 11-16 (2010).

[60] M. Kruk and M. Jaroniec, "Gas adsorption characterization of ordered organic-inorganic nanocomposite materials," *Chem. Mater.* **13,** 3169-3183 (2001).

[61] E. P. Barrett, L. G. Joyner and P. P. Halenda, "The determination of pore volume and area distributions in porous substances 1. Computations from nitrogen isotherms," *J. Am. Chem. Soc.* **73,** 373-380 (1951).

[62] J. C. Groen, L. A. A. Peffer and J. Pérez-Ramírez, "Pore size determination in modified micro- and mesoporous materials. Pitfalls and limitations in gas adsorption data analysis," *Micropor. Mesopor. Mat.* **60,** 1-17 (2003).

[63] S. Brunauer, P. H. Emmett and E. Teller, "Adsorption of gases in multimolecular layers," *J. Am. Chem. Soc.* **60,** 309-319 (1938).

[64] K. Morishige, N. Tateishi and S. Fukuma, "Capillary condensation of nitrogen in MCM-48 and SBA-16," *J. Phys. Chem. B* **107,** 5177-5181 (2003).

[65] J. Riikonen, J. Salonen and V. P. Lehto, "Utilising thermoporometry to obtain new insights into nanostructured materials – Review part 1," *J. Therm. Anal. Calorim.* **105,** 823-830 (2010).

[66] J. Riikonen, J. Salonen and V. P. Lehto, "Utilising thermoporometry to obtain new insights into nanostructured materials – Review part 2," *J. Therm. Anal. Calorim.* **105,** 821 (2010).

[67] A. H. Dessources, S. Hartmann, M. Baba, N. Huesing and J. M. Nedelec, "Multiscale characterization of hierarchically organized porous hybrid materials," *J. Mat. Chem.* **22,** 2713-2720 (2012).

[68] M. Brun, A. Lallemand, J. Quinson and C. Eyraud, "A new method for simultaneous determination of size and shape of pores: the thermoporometry," *Thermochim. Acta* **21,** 59-88 (1977).

[69] H. K. Christenson, "Confinement effects on freezing and melting," *J. Phys. Condens. Matter* **13,** R95-R133 (2001).

[70] R. Denoyel and R. J. M. Pellenq, "Simple phenomenological models for phase transitions in a confined geometry. 1: Melting and solidification in a cylindrical pore," *Langmuir* **18,** 2710-2716 (2002).

[71] K. Morishige, H. Yasunaga and Y. Matsutani, "Effect of pore shape on freezing and melting temperatures of water," *J. Phys. Chem. C* **114,** 4028-4035 (2010).

[72] R. J. M. Pellenq, B. Coasne, R. O. Denoyel and O. Coussy, "Simple phenomenological model for phase transitions in confined Geometry. 2. Capillary condensation/evaporation in cylindrical mesopores," *Langmuir* **25,** 1393-1402 (2009).

[73] V. V. Turov and R. Leboda, "Application of ^{1}H NMR spectroscopy method for determination of characteristics of thin layers of water adsorbed on the surface of dispersed and porous adsorbents," *Adv. Colloid Interface Sci.* **79,** 173-211 (1999).

[74] A. Bensaid, G. Patrat, M. Brunel, F. de Bergevin and R. Hérino, "Characterization of porous silicon layers by grazing- incidence X-ray fluorescence and diffraction," *Solid State Commun.* **79,** 923-928 (1991).

[75] D. Buttard, D. Bellet, G. Dolino and T. Baumbach, "X-ray diffuse scattering of p-type porous silicon," *J. Appl. Phys.* **91,** 2742-2752 (2002).

[76] Y. Ogata, H. Niki, T. Sakka and M. Iwasaki, "Oxidation of porous silicon under water vapor environment," *J. Electrochem. Soc.* **142,** 1595-1601 (1995).

[77] S. Guha, P. Steiner and W. Lang, "Resonant Raman scattering and photoluminescence studies of porous silicon membranes," *J. Appl. Phys.* **79,** 8664-8668 (1996).

[78] A. Steel, S. W. Carr and M. W. Anderson, "29Si solid-state NMR study of mesoporous M41S materials," *Chem. Mater.* **7,** 1829-1832 (1995).

[79] D. C. Monkhouse and J. L. Lach, "Use of adsorbents in enhancement of drug dissolution. I." *J. Pharm. Sci.* **61,** 1430-1435 (1972).

[80] M. Vallet-Regi, A. Ramila, R. P. del Real and J. Perez-Pariente, "A new property of MCM-41: Drug delivery system," *Chem. Mater.* **13,** 308-311 (2001).

[81] J. Salonen, L. Laitinen, A. Kaukonen, J. Tuura, M. Björkqvist, T. Heikkilä, K. Vähä-Heikkilä, J. Hirvonen and V. P. Lehto, "Mesoporous silicon microparticles for oral drug delivery: Loading and release of five model drugs," *J. Controlled Release* **108,** 362-374 (2005).

[82] J. M. Rosenholm, E. Peuhu, J. E. Eriksson, C. Sahlgren and M. Lindén, "Targeted intracellular delivery of hydrophobic agents using mesoporous hybrid silica nanoparticles as carrier systems," *Nano Lett.* **9,** 3308-3311 (2009).

[83] D. R. Radu, C. Y. Lai, K. Jeftinija, E. W. Rowe, S. Jeftinija and V. S. Y. Lin, "A polyamidoamine dendrimer-capped

mesoporous silica nanosphere-based gene transfection reagent," *J. Am. Chem. Soc.* **126,** 13216-13217 (2004).

[84] A. B. Foraker, R. J. Walczak, M. H. Cohen, T. A. Boiarski, C. F. Grove and P. W. Swaan, "Microfabricated porous silicon particles enhance paracellular delivery of insulin across intestinal Caco-2 cell monolayers," *Pharm. Res.* **20,** 110-116 (2003).

[85] I. I. Slowing, B. G. Trewyn and V. S. Y. Lin, "Mesoporous silica nanoparticles for intracellular delivery of membrane-impermeable proteins," *J. Am. Chem. Soc.* **129,** 8845-8849 (2007).

[86] T. Limnell, H. A. Santos, E. Mäkilä, T. Heikkilä, J. Salonen, D. Y. Murzin, N. Kumar, T. Laaksonen, L. Peltonen and J. Hirvonen, "Drug delivery formulations of ordered and nonordered mesoporous silica: Comparison of three drug loading methods," *J. Pharm. Sci.* **100,** 3294-3306 (2011).

[87] R. Mellaerts, J. A. G. Jammaer, M. Van Speybroeck, H. Chen, J. Van Humbeeck, P. Augustijns, G. Van den Mooter and J. A. Martens, "Physical state of poorly water soluble therapeutic molecules loaded into SBA-15 ordered mesoporous silica carriers: A case study with itraconazole and ibuprofen," *Langmuir* **24,** 8651-8659 (2008).

[88] J. R. Regalbuto, *Catalyst Preparation: Science and Engineering* (Taylor & Francis, Boca Raton, 2007).

[89] Y. Zhang, Z. Zhi, T. Jiang, J. Zhang, Z. Wang and S. Wang, "Spherical mesoporous silica nanoparticles for loading and release of the poorly water-soluble drug telmisartan," *J. Controlled Release* **145,** 257-263 (2010).

[90] P. Kinnari, E. Mäkilä, T. Heikkilä, J. Salonen, J. Hirvonen and H. A. Santos, "Comparison of mesoporous silicon and non-ordered mesoporous silica materials as drug carriers for itraconazole," *Int. J. Pharm.* **414,** 148-156 (2011).

[91] F. Kiekens, S. Eelen, L. Verheyden, T. Daems, J. Martens and G. van den Mooter, "Use of ordered mesoporous silica

to enhance the oral bioavailability of ezetimibe in dogs," *J. Pharm. Sci.* **101,** 1136-1144 (2012).

[92] T. Limnell, T. Heikkilä, H. A. Santos, S. Sistonen, S. Hellstén, T. Laaksonen, L. Peltonen, N. Kumar, D. Y. Murzin, M. Louhi-Kultanen, J. Salonen, J. Hirvonen and V. P. Lehto, "Physicochemical stability of high indomethacin payload ordered mesoporous silica MCM-41 and SBA-15 microparticles," *Int. J. Pharm.* **416,** 242-251 (2011).

[93] K. L. Jarvis, T. J. Barnes and C. A. Prestidge, "Surface chemical modification to control molecular interactions with porous silicon," *J. Colloid Interface Sci.* **363,** 327-333 (2011).

[94] A. P. Mann, T. Tanaka, A. Somasunderam, X. Liu, D. G. Gorenstein and M. Ferrari, "E-selectin-targeted porous silicon particle for nanoparticle delivery to the bone marrow," *Adv. Mater.* **23,** H278-H282 (2011).

[95] V. P. Lehto, K. Vähä-Heikkilä, J. Paski and J. Salonen, "Use of thermoanalytical methods in quantification of drug load in mesoporous silicon microparticles," *J. Therm. Anal. Calorim.* **80,** 393-397 (2005).

[96] M. Alcoutlabi and G. B. McKenna, "Effects of confinement on material behaviour at the nanometre size scale," *J. Phys. Condens. Matter* **17,** R461-R524 (2005).

[97] F. Wang, H. Hui, T. J. Barnes, C. Barnett and C. A. Prestidge, "Oxidized mesoporous silicon microparticles for improved oral delivery of poorly soluble drugs," *Mol. Pharmaceutics* **7,** 227-236 (2010).

[98] V. Ambrogi, L. Perioli, F. Marmottini, S. Giovagnoli, M. Esposito and C. Rossi, "Improvement of dissolution rate of piroxicam by inclusion into MCM-41 mesoporous silicate," *Eur. J. Pharm. Sci.* **32,** 216-222 (2007).

[99] V. Ambrogi, L. Perioli, C. Pagano, F. Marmottini, M. Ricci, A. Sagnella and C. Rossi, "Use of SBA-15 for furosemide

oral delivery enhancement," *Eur. J. Pharm. Sci.* **46,** 43-48 (2012).

[100] B. D. Hamilton, J. -. Ha, M. A. Hillmyer and M. D. Ward, "Manipulating crystal growth and polymorphism by confinement in nanoscale crystallization chambers," *Acc. Chem. Res.* **45,** 414-423 (2012).

[101] S. C. Shen, W. K. Ng, L. Chia, J. Hu and R. B. H. Tan, "Physical state and dissolution of ibuprofen formulated by co-spray drying with mesoporous silica: Effect of pore and particle size," *Int. J. Pharm.* **410,** 188-195 (2011).

[102] K. L. Jarvis, T. J. Barnes and C. A. Prestidge, "Thermal oxidation for controlling protein interactions with porous silicon," *Langmuir* **26,** 14316-14322 (2010).

[103] C. Washington, "Drug release from microdisperse systems: A critical review," *Int. J. Pharm.* **58,** 1-12 (1990).

[104] T. Heikkilä, J. Salonen, J. Tuura, N. Kumar, T. Salmi, D. Y. Murzin, M. S. Hamdy, G. Mul, L. Laitinen, A. Kaukonen, J. Hirvonen and V. P. Lehto, "Evaluation of mesoporous TCPSi, MCM-41, SBA-15, and TUD-1 materials as API carriers for oral drug delivery," *Drug Deliv.* **15,** 337-347 (2007).

[105] R. Mellaerts, R. Mols, P. Kayaert, P. Annaert, J. Van Humbeeck, G. Van den Mooter, J. A. Martens and P. Augustijns, "Ordered mesoporous silica induces pH-independent supersaturation of the basic low solubility compound itraconazole resulting in enhanced transepithelial transport," *Int. J. Pharm.* **357,** 169-179 (2008).

[106] B. C. Hancock and M. Parks, "What is the true solubility advantage for amorphous pharmaceuticals?" *Pharm. Res.* **17,** 397-404 (2000).

[107] R. H. Müller and K. Peters, "Nanosuspensions for the formulation of poorly soluble drugs. I. Preparation by a size-reduction technique," *Int. J. Pharm.* **160,** 229-237 (1998).

[108] C. M. Keck and R. H. Müller, "Drug nanocrystals of poorly soluble drugs produced by high pressure homogenisation," *Eur. J. Pharm. Biopharm.* **62,** 3-16 (2006).

[109] M. Mosharraf, T. Sebhatu and C. Nyström, "The effects of disordered structure on the solubility and dissolution rates of some hydrophilic, sparingly soluble drugs," *Int. J. Pharm.* **177,** 29-51 (1999).

[110] S. Wang, "Ordered mesoporous materials for drug delivery," *Micropor. Mesopor. Mat.* **117,** 1-9 (2009).

[111] C. A. Prestidge, T. J. Barnes, A. Mierczynska-Vasilev, W. Skinner, F. Peddie and C. Barnett, "Loading and release of a model protein from porous silicon powders," *Phys. Status Solidi A* **204,** 3361-3366 (2007).

[112] V. Hlady and J. Buijs, "Protein adsorption on solid surfaces," *Curr. Opin. Biotechnol.* **7,** 72-77 (1996).

[113] T. Asefa, A. N. Otuonye, G. Wang, E. A. Blair, R. Vathyam and K. Denton, "Controlling adsorption and release of drug and small molecules by organic functionalization of mesoporous materials," *Adsorption* **15,** 287-299 (2009).

[114] K. L. Jarvis, T. J. Barnes and C. A. Prestidge, "Surface chemistry of porous silicon and implications for drug encapsulation and delivery applications," *Adv. Colloid Interface Sci.* **175,** 25-38 (2012).

[115] S. W. Song, K. Hidajat and S. Kawi, "Functionalized SBA-15 materials as carriers for controlled drug delivery: Influence of surface properties on matrix-drug interactions," *Langmuir* **21,** 9568-9575 (2005).

[116] B. Munoz, A. Ramila, J. Perez-Pariente, I. Diaz and M. Vallet-Regi, "MCM-41 organic modification as drug delivery rate regulator," *Chem. Mater.* **15,** 500-503 (2003).

[117] J. Andersson, J. Rosenholm, S. Areva and M. Linden, "Influences of material characteristics on ibuprofen drug loading and release profiles from ordered micro- and

mesoporous silica matrices," *Chem. Mater.* **16,** 4160-4167 (2004).

[118] T. Ukmar, U. Maver, O. Planinšek, V. Kaučič, M. Gaberšček and A. Godec, "Understanding controlled drug release from mesoporous silicates: Theory and experiment," *J. Controlled Release* **155,** 409-417 (2011).

[119] M. Van Speybroeck, R. Mols, R. Mellaerts, T. D. Thi, J. A. Martens, J. V. Humbeeck, P. Annaert, G. V. D. Mooter and P. Augustijns, "Combined use of ordered mesoporous silica and precipitation inhibitors for improved oral absorption of the poorly soluble weak base itraconazole," *Eur. J. Pharm. Biopharm.* **75,** 354-365 (2010).

[120] M. Van Speybroeck, R. Mellaerts, R. Mols, T. D. Thi, J. A. Martens, J. Van Humbeeck, P. Annaert, G. Van den Mooter and P. Augustijns, "Enhanced absorption of the poorly soluble drug fenofibrate by tuning its release rate from ordered mesoporous silica," *Eur. J. Pharm. Sci.* **41,** 623-630 (2010).

[121] M. van Speybroeck, R. Mellaerts, T. D. Thi, J. A. Martens, J. Van Humbeeck, P. Annaert, G. Van den Mooter and P. Augustijns, "Preventing release in the acidic environment of the stomach via occlusion in ordered mesoporous silica enhances the absorption of poorly soluble weakly acidic drugs," *J. Pharm. Sci.* **100,** 4864-4876 (2011).

[122] Y. Zhang, J. Wang, X. Bai, T. Jiang, Q. Zhang and S. Wang, "Mesoporous silica nanoparticles for increasing the oral bioavailability and permeation of poorly water soluble drugs," *Mol. Pharmaceutics* **9,** 505-513 (2012).

[123] X. Xia, C. Zhou, L. Ballell and A. E. Garcia-Bennett, "In vivo enhancement in bioavailability of atazanavir in the presence of proton-pump inhibitors using mesoporous materials," *ChemMedChem* **7,** 43-48 (2012).

[124] F. Tang, L. Li and D. Chen, "Mesoporous silica nanoparticles: Synthesis, biocompatibility and drug delivery," *Adv. Mater.* **24,** 1504-1534 (2012).

[125] A. Suwalski, H. Dabboue, A. Delalande, S. F. Bensamoun, F. Canon, P. Midoux, G. Saillant, D. Klatzmann, J. Salvetat and C. Pichon, "Accelerated Achilles tendon healing by PDGF gene delivery with mesoporous silica nanoparticles," *Biomaterials* **31,** 5237-5245 (2010).

[126] J. Lu, M. Liong, Z. Li, J. I. Zink and F. Tamanoi, "Biocompatibility, biodistribution, and drug-delivery efficiency of mesoporous silica nanoparticles for cancer therapy in animals," *Small* **6,** 1794-1805 (2010).

[127] M. Kovalainen, J. Mönkäre, E. Mäkilä, J. Salonen, V. P. Lehto, K. H. Herzig and K. Järvinen, "Mesoporous Silicon (PSi) for Sustained Peptide Delivery: Effect of PSi Microparticle Surface Chemistry on Peptide YY3-36 Release," *Pharm. Res.* **29,** 837-846 (2012).

[128] M. Kilpeläinen, J. Mönkäre, M. A. Vlasova, J. Riikonen, V. P. Lehto, J. Salonen, K. Järvinen and K. H. Herzig, "Nanostructured porous silicon microparticles enable sustained peptide (Melanotan II) delivery," *Eur. J. Pharm. Biopharm.* **77,** 20-25 (2011).

[129] Y. Fukuda, Y. Yingda, W. Zhou, K. Furuya and H. Suzuki, "Quenching of porous silicon photoluminescence by ammonia hydrogen peroxide mixture," *J. Electrochem. Soc.* **147,** 3914-3916 (2000).

[130] H. L. Li, Y. Zhu, D. Xu, Y. Wan, L. Xia and X. S. Zhao, "Vapor-phase silanization of oxidized porous silicon for stabilizing composition and photoluminescence," *J. Appl. Phys.* **105,** 114307-1-114307-7 (2009).

[131] A. E. Pap, K. Kordás, T. F. George and S. Leppävuori, "Thermal oxidation of porous silicon: Study on reaction kinetics," *J. Phys. Chem. B* **108,** 12744-12747 (2004).

[132] G. H. Findenegg, S. Jaehnert, D. Akcakayiran and A. Schreiber, "Freezing and Melting of Water Confined in Silica Nanopores," *ChemPhysChem* **9,** 2651-2659 (2008).

[133] T. Azais, C. Tourne-Peteilh, F. Aussenac, N. Baccile, C. Coelho, J. Devoisselle and F. Babonneau, "Solid-state NMR study of ibuprofen confined in MCM-41 material," *Chem. Mater.* **18,** 6382-6390 (2006).

[134] F. Qian, N. Ni, L. S. Burton, Y. F. Wang, S. Desikan, M. Hussain and R. L. Smith, "Sustained release subcutaneous delivery of BMS-686117, a GLP-1 receptor peptide agonist, via a zinc adduct," *Int. J. Pharm.* **374,** 46-52 (2009).

[135] Y. Tang and J. Singh, "Thermosensitive drug delivery system of salmon calcitonin: In vitro release, in vivo absorption, bioactivity and therapeutic efficacies," *Pharm. Res.* **27,** 272-284 (2010).

[136] M. Kaasalainen, E. Mäkilä, J. Riikonen, M. Kovalainen, K. Järvinen, K. H. Herzig, V. P. Lehto and J. Salonen, "Effect of isotonic solutions and peptide adsorption on zeta potential of porous silicon nanoparticle drug delivery formulations," *Int. J. Pharm.* **431,** 230-236 (2012).

Joakim Riikonen

Modification, Characterization and Applications of Mesoporous Silicon-Based Drug Carriers

Mesoporous silicon and silica are materials consisting of small pores with diameters between 2 and 50 nm. These materials exhibit high potential as drug carriers, since they are able to improve the delivery characteristics of drugs loaded inside the pores. The present thesis investigates the development of these materials for drug delivery applications. Modifications to the surface chemistry as well as modifications and characterization of the pore structure were studied. In addition, the physical state of drugs inside the pores was investigated. Finally, it was shown that porous silicon microparticles could be used to sustain the delivery of peptides in a biologically active form *in vivo*.

UNIVERSITY OF
EASTERN FINLAND

Publications of the University of Eastern Finland
Dissertations in Forestry and Natural Sciences

ISBN 978-952-61-0894-0